

Distributionally Robust Formulation and Model Selection for the Graphical Lasso

Pedro Cisneros-Velarde¹, Sang-Yun Oh², Alexander Petersen²
 Center for Control, Dynamical Systems and Computation¹,
 Department of Statistics and Applied Probability²,
 University of California, Santa Barbara

Abstract

Building on a recent framework for distributionally robust optimization in machine learning, we develop a similar framework for estimation of the inverse covariance matrix for multivariate data. We provide a novel notion of a Wasserstein ambiguity set specifically tailored to this estimation problem, from which we obtain a representation for a tractable class of regularized estimators. Special cases include penalized likelihood estimators for Gaussian data, specifically the graphical lasso estimator. As a consequence of this formulation, a natural relationship arises between the radius of the Wasserstein ambiguity set and the regularization parameter in the estimation problem. Using this relationship, one can directly control the level of robustness of the estimation procedure by specifying a desired level of confidence with which the ambiguity set contains a distribution with the true population covariance. Furthermore, a unique feature of our formulation is that the radius can be expressed in closed-form as a function of the ordinary sample covariance matrix. Taking advantage of this finding, we develop a simple algorithm to determine a regularization parameter for graphical lasso, using only the bootstrapped sample covariance matrices, meaning that computationally expensive repeated evaluation of the graphical lasso algorithm is not necessary. Alternatively, the distributionally robust formulation can also quantify the robustness of the corresponding estimator if one uses an off-the-shelf method such as cross-validation. Finally, we numerically study the obtained regularization criterion and analyze the robustness of other automated tuning procedures used in practice.

1 Introduction

In statistics and machine learning, the covariance matrix Σ of a random vector $X \in \mathbb{R}^d$ is a fundamental quantity for characterizing marginal pairwise dependencies between variables. Furthermore, the inverse covariance matrix $\Omega = \Sigma^{-1}$ provides information about the *conditional* dependency structure between the variables when X is Gaussian. In this case, $\Omega_{jk} = 0$ if and only if the j th and k th variables of X are conditionally independent given the rest. Such relationships are of interest in many applications such as environmental science, biology, and neuroscience [11, 13, 18], and have given rise to various statistical and machine learning methods for inverse covariance estimation.

Given an iid sample $X_i \sim X$, $i = 1, \dots, n$, the sample covariance $A_n = \frac{1}{n} \sum_{i=1}^n X_i X_i^\top$, which is the maximum likelihood estimator if X is Gaussian, can be a poor estimator of Σ unless d/n is very small. Driven by a so-called high dimensional setting where $n \ll d$, where A_n is not invertible, regularized estimation of the precision matrix has gained significant interest [6, 8, 10, 17, 32, 36]. Such regularization procedures are useful even when A_n is a stable estimate (i.e., positive definite with small condition number), since the inverse covariance estimate A_n^{-1} is dense and will not reflect the sparsity of corresponding nonzero elements in Ω .

Distributionally Robust Optimization: Let \mathbb{S}_d be the set of $d \times d$ symmetric matrices, and $\mathbb{S}_d^{++} \subset \mathbb{S}_d$ be the subset of positive definite symmetric matrices. Given a loss function $l(X; K)$ for $K \in \mathbb{S}_d^{++}$ and $X \in \mathbb{R}^d$, a classical approach would be to estimate Ω by minimizing the empirical loss $\sum_{i=1}^n l(X_i; K)$ over $K \in \mathbb{S}_d^{++}$, perhaps including a regularization or penalty term. The error in this estimate arises from the discrepancy between the true data-generating distribution and the observed training samples, and can be assessed by

various tools such as concentration bounds or rates of convergence. In contrast, *distributionally robust optimization* (DRO) is a technique that explicitly incorporates uncertainty about the distribution of the X_i into the estimation procedure. For an introduction on the general topic of DRO, we refer to the works [28, 3] and the references therein. In the context of inverse covariance estimation, a distributionally robust estimate of Ω is obtained by solving

$$\inf_{K \in \mathbb{S}_d^{++}} \sup_{P \in \mathcal{S}} E_P[l(K; X)], \quad (1)$$

where \mathcal{S} , known as an *ambiguity set*, is a collection of probability measures on \mathbb{R}^d . As pointed out in [3], a natural choice for \mathcal{S} is the neighborhood $\{P \mid D(P, \mu) \leq \delta\}$, with μ being a chosen baseline model, δ being some tolerance level which defines the uncertainty size of the ambiguity set, and D being some discrepancy metric between two probability measures. In a practical setting, we have access to some samples (or data points) from the unknown distribution, and thus, a good candidate for the baseline model is the empirical measure.

Very recent work in [23], also analyzed in [4], used the DRO framework to construct a new regularized (dense) inverse covariance estimator. Working under the assumption that X is Gaussian, the authors construct an ambiguity set \mathcal{S} of Gaussian distributions that, up to a certain tolerance level, are consistent with the observed data. Recent work on DRO in other machine learning problems has revealed explicit connections to well-known regularized estimators, specifically regularized logistic regression [28] and the square-root lasso for linear models [2]; however, such a connection to regularized *sparse* inverse covariance estimators that are used in practice has yet to be made.

The Graphical Lasso: One of the most common methods to recover the sparsity pattern in Ω is to add an l_1 -regularization term to the Gaussian likelihood function, motivated by the consideration of the *Gaussian Graphical Model* (GGM). A sparse estimate of $\Omega = \Sigma^{-1}$ is produced by minimizing

$$\mathcal{L}_\lambda(K) = \frac{1}{n} \sum_{i=1}^n X_i^\top K X_i - \log |K| + \lambda \sum_{i=1}^d \sum_{j=1}^d |k_{ij}|, \quad (2)$$

where k_{ij} is the (i, j) entry of K and $\lambda > 0$ is a user-specified regularization parameter [1, 10, 36]. Although several algorithms exist to solve this objective function [10, 26, 12], the minimizer of (2) is often referred to as *graphical lasso* estimator [10]. The first two terms of (2) are related to Stein's loss [15] when evaluated at the empirical measure, and also correspond to the negative log-likelihood up to an additive constant if X is Gaussian. The performance of the graphical lasso estimator in high-dimensional settings has been investigated [27, 16], as well as modifications and extensions that implement some notion of *robustness*, i.e., for making it robust to outliers or relaxing the normality assumptions in the data [17, 19, 20, 33, 34].

Besides its theoretical relevance, the graphical lasso and its extensions also enjoy many practical advantages. For example, it has been used as a network inference tool. In these applications, the precision matrix can indicate which nodes in a network are conditionally independent given information from remaining nodes, thus giving an indication of network functionality. This has been important in neuroscience applications when studying the inference of brain connectivity [35, 29, 13]. Applications in gene regulatory networks and metabolomics have also been reported [22, 31, 18].

The performance of the graphical lasso estimator hinges critically on the choice of λ . While there have been studies on how to properly tune λ to obtain a consistent estimator or to establish correct detection of nonzero elements in the precision matrix [27, 1, 21],

in practice, this selection is often made through automated methods like cross-validation.

Contributions: In this paper, we propose a distributionally robust reformulation of the graphical lasso estimator in (2). Following [28, 2, 9], we utilize the Wasserstein metric to quantify distributional uncertainty for the construction of the ambiguity set. The following points summarize our main contributions.

- We propose a novel definition of ambiguity set specifically designed for inverse covariance estimation, leading to a tractable class of DRO problems corresponding to ℓ_p -norm regularized estimators. This formulation provides a natural relationship between the size of the ambiguity set and the regularization parameter in the estimation problem. As the graphical lasso estimator (2) is a special case, this provides us with a new interpretation of this popular technique.
- We use this formulation to suggest a criterion for the selection of the regularization parameter in the estimation problem in the classical regime $n > d$. This criterion follows the *Robust Wasserstein*

Profile (RWP) inference recently introduced in [2], which makes no assumption on the normality of the data, and which we tailor to our specific problem. The proposed criterion expresses the regularization parameter as an explicit function of the sample covariance A_n , unlike other instances where RWP has been implemented which rely on stochastic dominance arguments.

- We formulate a novel *robust selection* (RobSel) algorithm for regularization parameter choice. Focusing on the graphical lasso, we provide numerical results that compare the performance of cross-validation, our proposed algorithm, and another automated tuning procedure [1] for the selection of the regularization term.

The paper is organized as follows. In Section 2 we describe our main theoretical result: the distributionally robust formulation of the regularized inverse covariance (log-likelihood) estimation, from which graphical lasso is a particular instance. In Section 3 we propose a criterion for choosing the regularization parameter inspired by this formulation and outline the bootstrap-based RobSel algorithm for its computation. In Section 4 we present some numerical results comparing the proposed criterion of Section 3 with cross-validation and another method found in the literature. Finally, we state some concluding remarks and future research directions in Section 5. All proofs of theoretical results can be found in the supplementary material.

2 A Distributionally Robust Formulation of the Graphical lasso

First, we provide preliminary details on notation. Given a matrix $A \in \mathbb{R}^{d \times d}$, a_{jk} denotes its (j, k) entry and $\text{vec}(A) \in \mathbb{R}^{d^2}$ denotes its vectorized form, which we assume to be in a row major fashion. For matrices denoted by Greek letters, its entries are simply denoted by appropriate subscripts, i.e. Σ_{jk} . The operator $|\cdot|$, when applied to a matrix, denotes its determinant; when applied to a scalar or a vector, it denotes the absolute value or entry-wise absolute value, respectively. The ℓ_p -norm of a vector is denoted by $\|\cdot\|_p$. We use the symbol \Rightarrow to denote convergence in distribution.

Recall that $X \in \mathbb{R}^d$ is a zero-mean random vector with covariance matrix $\Sigma \in \mathbb{S}_d^{++}$. Let \mathbb{Q}_0 be the probability law for X and $\Omega = \Sigma^{-1}$ be the precision matrix. Define the *graphical loss function* as

$$\begin{aligned} l(X; K) &= X^\top K X - \log |K| \\ &= \text{trace}(K X X^\top) - \log |K|. \end{aligned} \tag{3}$$

Then $E_{\mathbb{Q}_0}[l(K; X)] = \text{trace}(K \Sigma) - \log |K|$ is a convex function of K over the convex cone \mathbb{S}_d^{++} . Using the first-order optimality criterion, we observe that $K = \Omega$ sets the gradient $\frac{\partial}{\partial K} E_{\mathbb{Q}_0}[l(X; K)] = \Sigma - K^{-1}$ equal to the zero matrix (see [5, Appendix A] for details on this differentiation). Hence,

$$\arg \min_{C \in \mathbb{S}_d^{++}} E_{\mathbb{Q}_0}[l(X; K)] = \Omega.$$

so that (3) is a consistent loss function.

Now, if we consider an iid random sample $X_1, \dots, X_n \sim X$, $n > d$, with empirical measure \mathbb{Q}_n , then

$$\arg \min_{K \in \mathbb{S}_d^{++}} E_{\mathbb{Q}_n}[l(X; K)] = \arg \min_{K \in \mathbb{S}_d^{++}} \frac{1}{n} \sum_{i=1}^n l(X_i; K) = A_n^{-1}$$

with $A_n = \frac{1}{n} \sum_{i=1}^n X_i X_i^\top$. Thus, as described in the Introduction, a natural approach would be to implement the DRO procedure outlined in [9] by building an ambiguity set based on perturbations of \mathbb{Q}_n , leading to the DRO estimate given by (1). However, this approach does not convert (1) into a tractable optimization problem, since the inner supremum cannot be explicitly given in closed-form.

As an alternative, let \mathbb{P}_0 represent the measure of the random matrix XX^\top on \mathbb{S}_d induced by \mathbb{Q}_0 and, similarly let \mathbb{P}_n be empirical measure of the sample $W_i = X_i X_i^\top$, $i = 1, \dots, n$. Redefining the graphical loss function $l : \mathbb{S}_d \times \mathbb{S}_d^{++}$ as

$$l(W; K) = \text{trace}(K W) - \log |K|, \tag{4}$$

then

$$\Omega = \arg \min_{K \in \mathbb{S}_d^{++}} E_{\mathbb{P}_0}[l(W; K)], \quad A_n^{-1} = \arg \min_{K \in \mathbb{S}_d^{++}} E_{\mathbb{P}_n}[l(W; K)].$$

This observation leads to a tractable DRO formulation by constructing ambiguity sets built around the empirical measure \mathbb{P}_n . The DRO formulation for inverse covariance estimation becomes

$$\min_{K \in \mathbb{S}_d^{++}} \sup_{P: \mathcal{D}_c(P, \mathbb{P}_n) \leq \delta} E_P[l(W; K)]. \quad (5)$$

The ambiguity set in this formulation is specified by the collection of measures $\{P \mid \mathcal{D}_c(P, \mathbb{P}_n) \leq \delta\}$, which we now describe. Given two probability distributions P_1 and P_2 on \mathbb{S}_d and some transportation cost function $c: \mathbb{S}_d \times \mathbb{S}_d \rightarrow [0, \infty)$ (which we will specify below), we define the *optimal transport cost* between P_1 and P_2 as

$$\mathcal{D}_c(P_1, P_2) = \inf \{E_\pi [c(U, V)] \mid \pi \in \mathcal{P}(\mathbb{S}_d \times \mathbb{S}_d), \pi_U = P_1, \pi_V = P_2\}, \quad (6)$$

where $\mathcal{P}(\mathbb{S}_d \times \mathbb{S}_d)$ is the set of joint probability distributions π of (U, V) supported on $\mathbb{S}_d \times \mathbb{S}_d$, and π_U and π_V denote the marginals of U and V under π , respectively. In this paper, we are interested in cost functions

$$c(U, V) = \|\mathbf{vec}(U) - \mathbf{vec}(V)\|_q^\rho, \quad U, V \in \mathbb{S}_d, \rho \geq 1, q \in [1, \infty]. \quad (7)$$

As pointed out by [2], the resulting optimal transport cost $\mathcal{D}_c^{1/\rho}$ is the Wasserstein distance of order ρ . Our first theoretical result demonstrates that the optimization in (5) corresponds to a class of regularized estimators under the graphical loss function (4).

Theorem 2.1 (DRO formulation of regularized inverse covariance estimation). *Consider the cost function in (7) for a fixed $\rho \geq 1$. Then,*

$$\min_{K \in \mathbb{S}_d^{++}} \sup_{P: \mathcal{D}_c(P, \mathbb{P}_n) \leq \delta} E_P[l(W; K)] = \min_{K \in \mathbb{S}_d^{++}} \left\{ \text{trace}(KA_n) - \log|K| + \delta^{1/\rho} \|\mathbf{vec}(K)\|_p \right\}, \quad (8)$$

where $\frac{1}{p} + \frac{1}{q} = 1$.

Theorem 2.1 is a remarkable theoretical result that provides a mapping between the regularization parameter and the uncertainty size δ of the ambiguity set in the DRO formulation. Then, the regularization problem reduces to determining a good criterion for choosing δ , which we explore in Section 3. Moreover, we obtain the *graphical lasso* formulation (2) by setting $q = \infty$ in (7). From (8), a smaller ambiguity set implies less robustness being introduced in the estimation problem by reducing the importance of the regularization term. Conversely, a larger regularization term increases the number of nuisance distributions inside the ambiguity set, and thus the robustness.

Remark 2.2. *The ambiguity set used in (8) makes no assumptions on the normality of the distribution of the samples $\{X_1, \dots, X_n\}$. Then, (8) tells us that adding a penalization to the precision matrix gives a robustness in terms of the distributions that the samples may have, which do not necessarily have to be Gaussian for this formulation to hold. Furthermore, it holds independent of the relationship between n and d .*

3 Selection of the regularization parameter

This section follows closely the line of thought recently introduced by [2] in the analysis of regularized estimators under the DRO formulation. Specifically, we will demonstrate that the ambiguity set $\{P: \mathcal{D}_c(P, \mathbb{P}_n) \leq \delta\}$ represents a confidence region for $\Omega = \Sigma^{-1}$, and use the techniques of [2] to explicitly connect the ambiguity size δ with a confidence level. As previously stated, $l(W; K)$ is a differentiable function on $K \in \mathbb{S}_d^{++}$ with $\frac{\partial}{\partial K} l(W; K) = W - K^{-1}$, so that

$$E_{\mathbb{P}_0} \left[\frac{\partial}{\partial K} l(W; K) \Big|_{K=\Omega} \right] = \mathbb{0}_{d \times d}. \quad (9)$$

Hence, even though the loss function $l(W; K)$ has been inspired from the log-likelihood estimation of the covariance matrix Σ for samples of Gaussian random vectors, equation (9) is transparent to any underlying distribution of the data. For any $K \in \mathbb{S}_d^{++}$, define the set

$$\mathcal{O}(K) := \left\{ P \in \mathcal{P}(\mathbb{S}_d) \mid E_P \left[\frac{\partial}{\partial K'} l(W; K') \Big|_{K'=K} \right] = \mathbb{0}_{d \times d} \right\}, \quad (10)$$

corresponding to all probability measures with covariance K^{-1} , i.e. for which K is an optimal loss minimization parameter; here, $\mathcal{P}(\mathbb{S}_d)$ denotes the set of all probability distributions supported on \mathbb{S}_d . Thus, $\mathcal{O}(\Omega)$ contains all probability measures with covariance matrix agreeing with that of X .

Implicitly, the Wasserstein ambiguity set $\{P : \mathcal{D}_c(P, \mathbb{P}_n) \leq \delta\}$ is linked to the collection of covariance matrices

$$\begin{aligned} \mathcal{C}_n(\delta) &:= \{K \in \mathbb{S}_d^{++} \mid \text{there exists } P \in \mathcal{O}(K) \cap \{P \mid \mathcal{D}_c(P, \mathbb{P}_n) \leq \delta\}\} \\ &= \bigcup_{P: \mathcal{D}_c(P, \mathbb{P}_n) \leq \delta} \arg \min_{K \in \mathbb{S}_d^{++}} E_P[l(W; K)]. \end{aligned} \quad (11)$$

We refer to $\mathcal{C}_n(\delta)$ as the set of *plausible* selections for Ω .

Lemma 3.1 (Interchangeability in the DRO formulation). *Consider the setting of Theorem 2.1. Then, for $n > d$, the following holds with probability one:*

$$\inf_{K \in \mathbb{S}_d^{++}} \sup_{P: \mathcal{D}_c(P, \mathbb{P}_n) \leq \delta} E_P[l(W; K)] = \sup_{P: \mathcal{D}_c(P, \mathbb{P}_n) \leq \delta} \inf_{K \in \mathbb{S}_d^{++}} E_P[l(W; K)]. \quad (12)$$

Lemma 3.1 states that any estimator obtained by minimizing the left-hand side of (12) must be in $\mathcal{C}_n(\delta)$, otherwise the right-hand side of (12) would be strictly greater than the left. Thus, in line with the goal of providing a robust estimator, the idea is to choose δ so that $\mathcal{C}_n(\delta)$ also contains the true inverse covariance matrix Ω with high confidence.

As \mathbb{P}_0 is the weak limit of \mathbb{P}_n , we will eventually have that $\Omega \in \mathcal{C}_n(\delta)$ with high probability for any δ , so that $\mathcal{C}_n(\delta)$ is a confidence region for Ω . From this observation, we can choose the uncertainty size δ optimally by the criterion

$$\delta = \inf \{\delta > 0 \mid P(\Omega \in \mathcal{C}_n(\delta)) \geq 1 - \alpha\}, \quad (13)$$

i.e., for a specified confidence level $1 - \alpha$, we choose δ so that $\mathcal{C}_n(\delta)$ is a $(1 - \alpha)$ -confidence region for Ω .

To continue our analysis, we make use of the so-called *Robust Wasserstein Profile (RWP) function* R_n introduced by [2],

$$\begin{aligned} R_n(K) &= \inf \{\mathcal{D}_c(P, \mathbb{P}_n) \mid P \in \mathcal{O}(K)\} \\ &= \inf \left\{ \mathcal{D}_c(P, \mathbb{P}_n) \mid E_P \left[\frac{\partial}{\partial K'} l(W; K') \Big|_{K'=K} \right] = \mathbb{0}_{d \times d} \right\}, \end{aligned} \quad (14)$$

for $K \in \mathbb{S}_d^{++}$, which has the geometric interpretation of being the minimum distance between the empirical distribution and any distribution that satisfies the optimality condition for the precision matrix K . Then, using the equivalence of events $\{\Omega \in \mathcal{C}_n(\delta)\} = \{\mathcal{O}(\Omega) \cap \{P \mid \mathcal{D}_c(P, \mathbb{P}_n) \leq \delta\} \neq \emptyset\} = \{R_n(\Omega) \leq \delta\}$, (13) becomes equivalent to

$$\delta = \arg \inf \{\delta > 0 \mid P(R_n(\Omega) \leq \delta) \geq 1 - \alpha\}, \quad (15)$$

i.e., the optimal selection of δ is the $1 - \alpha$ quantile of $R_n(\Omega)$. Indeed, the set $\{P \mid \mathcal{D}_c(P, \mathbb{P}_n) \leq R_n(\Omega)\}$ is the smallest ambiguity set around the empirical measure \mathbb{P}_n such that there exists a distribution for which Ω is an optimal loss minimization parameter. In contrast to previously reported applications of the RWP function on linear regression and logistic regression [2], our problem allows for a (finite sample) closed form expression of this function. This is due to the fact that we have recast the covariance Σ as the mean of the random matrix XX^\top , so that the following result gives a nontrivial generalization of [2, Example 3].

Theorem 3.2 (RWP function). *Consider the cost function in (7) for a fixed $\rho \geq 1$. For $K \in \mathbb{S}_d^{++}$, consider $R_n(K)$ as in (14). Then,*

$$R_n(K) = \|\text{vec}(A_n - K^{-1})\|_q^\rho. \quad (16)$$

We now establish important convergence guarantees on the RWP function in the following corollary.

Corollary 3.3 (Asymptotic behavior of the RWP function). *Suppose that the conditions of Theorem 3.2 hold, and that $E_{Q_0}(\|X\|_2^4) < \infty$. Let $H \in \mathbb{S}_d$ be a matrix of jointly Gaussian random variables with zero mean and such that $\text{Cov}(h_{ij}, h_{k\ell}) = E[w_{ij}w_{k\ell}] - \Sigma_{ij}\Sigma_{k\ell} = E[x_i x_j x_k x_\ell] - \Sigma_{ij}\Sigma_{k\ell}$. Then,*

$$n^{\rho/2} R_n(\Omega) \Rightarrow \|\text{vec}(H)\|_q^\rho. \quad (17)$$

Proof. By the central limit theorem, we observe that $\sqrt{n}(A_n - \Sigma) \Rightarrow H$, and by the continuous mapping theorem, we get that

$$n^{\rho/2} R_n(\Omega) = \|\sqrt{n}\text{vec}(A_n - \Sigma)\|_q^\rho \Rightarrow \|\text{vec}(H)\|_q^\rho.$$

□

Remark 3.4. *Turning our attention back to Theorem 2.1, a robust selection for the ambiguity size or regularization parameter $\lambda = \delta^{1/\rho}$, as obtained from Theorem 3.2, is*

$$\delta^{1/\rho} = \inf \left\{ \delta > 0 \mid P(\|\text{vec}(A_n - \Sigma)\|_q \leq \delta) \geq 1 - \alpha \right\} \quad (18)$$

As a result, this robust selection for λ results in a class of estimators, given by minimizers of the right-hand side of (8), that are invariant to the choice of ρ in (7). Thus, for simplicity, we will set $\rho = 1$ in the remainder of the paper.

Remark 3.5. *Let $r_{1-\alpha}$ be the $(1 - \alpha)$ quantile from the distribution of the right-hand side of (17). Then, for any fixed α , the robust selection δ in (18) satisfies $n^{1/2}\delta \rightarrow r_{1-\alpha}$, so that the optimal decay rate of $n^{-1/2}$ for λ is automatically chosen by the RWP function.*

As solving (18) requires knowledge of Σ , we now outline the robust selection (RobSel) algorithm for data-adaptive choice of the regularization parameter δ for our inverse covariance estimation with an ℓ_p penalization parameter. The special case $p = 1$ corresponds to the graphical lasso in (2), in which case we will also use the notation $\delta = \lambda$. The asymptotic result in Corollary 3.3 invokes a central limit theorem, and thus motivates the approximation of the RWP function through bootstrapping, which we further explain and evaluate its numerical performance in the next section. Let $\alpha \in (0, 1)$ be a prespecified confidence level and B a large integer such that $(B + 1)(1 - \alpha)$ is also an integer.

Algorithm RobSel algorithm for estimation of the regularization parameter λ

- 1: For $b = 1, \dots, B$, obtain a bootstrap sample $X_{1b}^*, \dots, X_{nb}^*$ by sampling uniformly and with replacement from the data, and compute the bootstrap RWP function $R_{n,b}^* = \|A_{n,b}^* - A_n\|_q$, with the empirical covariance $A_{n,b}^*$ computed from the bootstrap sample.
- 2: Set λ to be the bootstrap order statistic $R_{n,((B+1)(1-\alpha))}^*$.

RobSel can potentially provide considerable computational savings over cross-validation in practice. Computing sample covariance matrices for each of B bootstrap samples has cost $O(Bnd^2)$. On the other hand, it is known that each iteration of graphical lasso can cost $O(d^3)$ in the worst case [21]; therefore, performing an F -fold cross-validation to search over L -grid of regularization parameters, each taking T -iterations of graphical lasso, would cost $O(FLTd^3)$.

4 Numerical results and analysis

The true precision matrix $\Omega \in \mathbb{S}_d^{++}$ used to generate simulated data has been constructed as follows. First, generate an adjacency matrix of an undirected Erdos-Renyi graph with equal edge probability and without self-loops. Then, the weight of each edge is sampled uniformly between $[0.5, 1]$, and the sign of each non-zero weight is positive or negative with equal probability of 0.5. Finally, the diagonal entries of this weighted adjacency matrix are set to 1 and the matrix is made diagonally dominant by following a procedure described in [24], which ensures that the resulting matrix Ω is positive definite. Throughout this numerical study section, a randomly generated sparse matrix Ω (edge probability 0.1 and $d = 100$) is fixed. Using this Ω , a

total of $N = 200$ datasets (of varying size n) were generated as independent observations from a multivariate zero-mean Gaussian distribution, i.e., $\mathcal{N}(\mathbf{0}_d, \Omega^{-1})$.

Consider the problem of choosing the regularization parameter λ (equivalently, the ambiguity size parameter δ) to obtain graphical lasso estimates \hat{K}_λ of Ω using the simulated datasets. An R software package, `glasso`, from CRAN was used throughout our numerical experiments section. Below, we compare three different criteria for choosing λ . The first criterion is *Robust Selection (RS)*, which follows our proposed RobSel algorithm with $B = 200$ sets of bootstrap samples. We present here results for $n > d$, but the results in the high-dimensional regime $n < d$ can be found in the supplementary material. The second criterion is the one proposed by *Banerjee et al. [1, Equation 3] (BN)*. The third criterion is a *5-fold cross-validation (CV)* procedure. The performance on the validation set is the evaluation of the graphical loss function under the empirical measure of the samples on the training set.

We compare model selection performance and parameter estimation performance of λ chosen by the three different approaches: λ_{RS} , λ_{BN} , and λ_{CV} . The following comparison metrics are used:

- *True positive rate (TPR) and false positive rate (FPR)*: TPR is the proportion of nonzero entries of Ω that are correctly identified in \hat{K}_λ , and FPR is the proportion of zero entries of Ω that are incorrectly identified as nonzeros in \hat{K}_λ .
- *Matthew's Correlation Coefficient (MCC)*: MCC summarizes all counts in the confusion matrix (TP, TN, FP and FN) in contrast to other measures like TPR and FPR. More details about MCC is given in supplemental subsection C.1.
- *Stein's loss*: $\text{trace}(\Omega^{-1}\hat{K}_\lambda) - \log|\Omega^{-1}\hat{K}_\lambda| - d$, which is zero whenever $\hat{K}_\lambda = \Omega$.
- *Difference of inverse covariances*: $\frac{\|\hat{K}_\lambda - \Omega\|_F}{d}$.
- *Out of sample loss*: We obtain a new sample, $X_1, \dots, X_{\lceil n/3 \rceil} \sim \mathcal{N}(\mathbf{0}_d, \Omega^{-1})$ and compute $\text{trace}(\hat{K}_\lambda \frac{1}{\lceil n/3 \rceil} \sum_{i=1}^{\lceil n/3 \rceil} X_i X_i^\top) - \log|\hat{K}_\lambda|$.

In the remainder of this section, we compare the model selection performance (FPR, TPR, MCC) and parameter estimation performance (Stein's loss, difference of inverse covariances, and out of sample loss) from our simulation results. As mentioned in Remark 3.5, supplemental subsection C.2 shows that λ_{RS} decrease as n increases as is also observed to be true with λ_{CV} and λ_{BN} . Furthermore, across the tested range of α , the regularization λ_{RS} are all larger than λ_{CV} for any n . Then, our distributionally robust representation (8) allows us to observe that even for small values of n , CV always chooses a λ that corresponds to smaller ambiguity sets than RS and BN.

To assess the accuracy of RobSel in estimating $\lambda = \delta$ for a given α , we approximated the right-hand side of (18) using the $N = 200$ data sets and the true covariance Σ , giving the “true” value λ_{RWP} . Figures in supplemental subsection C.3 show that the performance obtained by λ_{RWP} is similar to the one obtained by λ_{RS} for all comparison metrics. This finite sample behavior of RS indicates that the RobSel bootstrap algorithm reliably approximates the desired robustness level corresponding to the choice of α . These plots also indicate that the RS and BN criteria are more conservative than CV in achieving a lower FPR across different sample sizes, due to providing larger values for λ (see subsection C.2). In fact, this behavior of BN is as expected by [1, Theorem 2]. In terms of the other comparison metrics, the RS criterion gives better performance than BN.

Moreover, the trade-off between the preference for robustness and the preference for a higher density estimation of nonzero entries in the precision matrix can be observed in terms of the Matthews correlation coefficient (MCC), as shown in Fig. 1 and Table 1 in supplemental subsection C.1. Higher values in the curve of MCC implies values of λ that describe a better classification of the entries of Ω as either zero or nonzero (see subsection C.1 for more details). We observe that CV is placed at the left of the optimal value of the MCC and its under-performance is due to the overestimation of nonzero entries in Ω . On the other hand, RS is to the right of the optimal value and its under-performance is due to its conservative overestimation of zero entries in Ω induced by its robust nature. Then, it is up to the experimenter to know which method to use depending on whether she desires to control for the overestimation of zero or nonzero entries. Remarkably, for large numbers of n , RS seems to be much closer to the optimal performance than CV, i.e., maintains a lower false positive rate compared to CV while increasing the true positive rate.

Our results from the MCC analysis and subsection C.2 also indicate that we should aim for higher values of α if we want a performance closer to CV when using the RS criterion. In contrast, if we want more conservative results, we should aim for lower values of α . This is the power behind RS: it allows the use

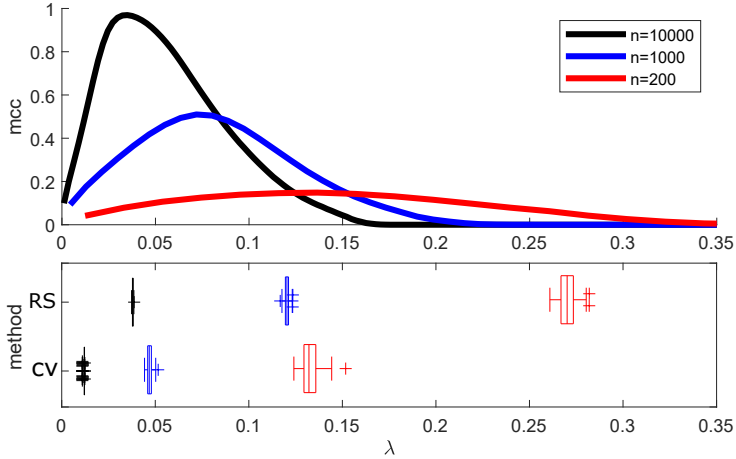


Figure 1: Matthews correlation coefficient (MCC) for three different sample sizes. The curves in the upper plot are the average MCC obtained over $N = 200$ datasets. The lower plot are boxplots for the CV and RS (with parameter $\alpha = 0.9$) methods for the different choices of n .

of a single parameter $\alpha \in (0, 1)$ to adjust the importance of the regularization term. This has a practical importance. CV is more computationally expensive as the dimension of the data and/or the length of the search grid for the optimal λ increases since it requires that the entire graphical lasso solution path be computed. Thus, RS can provide a candidate for λ with much lower computational cost.

5 Conclusion

We provide a recharacterization of the popular graphical lasso estimator in (2) as the optimal solution to a distributionally robust optimization problem. To the best of our knowledge, this is the first work to make such a connection for sparse inverse covariance estimation. The DRO form of the estimator leads to a reinterpretation of the regularization parameter as the radius of the distributional ambiguity set, which can be chosen based on a desired level of robustness. We propose the RobSel method for the selection of the regularization parameter and compare it to cross-validation for the graphical lasso. As the sample size increases, performance metrics for the two are similar. However, RobSel is a computationally simpler procedure, notably only performing the graphical lasso algorithm once at the final step rather than repeatedly as is necessary for cross-validation. Future work includes theoretical justification for robust selection of the regularization parameter for the graphical lasso in the high-dimensional setting.

References

- [1] Onureena Banerjee, Laurent El Ghaoui, and Alexandre d’Aspremont. Model selection through sparse maximum likelihood estimation for multivariate Gaussian or binary data. *J. Mach. Learn. Res.*, 9:485–516, 2008.
- [2] Jose Blanchet, Yank Kang, and Karthyek Murthy. Robust Wasserstein profile inference and applications to machine learning. 2016.
- [3] Jose Blanchet and Karthyek Murthy. Quantifying distributional model risk via optimal transport. 2016.
- [4] Jose Blanchet and Nian Si. Optimal uncertainty size in distributionally robust inverse covariance estimation. 2019.
- [5] S. Boyd and L. Vandenberghe. *Convex Optimization*. Cambridge University Press, 2004.

[6] Tony Cai, Weidong Liu, and Xi Luo. A constrained ℓ_1 minimization approach to sparse precision matrix estimation. *Journal of the American Statistical Association*, 106(494):594–607, jun 2011.

[7] Davide Chicco. Ten quick tips for machine learning in computational biology. *BioData Mining*, 10(1):35, Dec 2017.

[8] David Edwards. *Introduction to Graphical Modelling*. Springer-Verlag New York, 2010.

[9] Peyman Mohajerin Esfahani and Daniel Kuhn. Data-driven distributionally robust optimization using the Wasserstein metric: Performance guarantees and tractable reformulations. *Mathematical Programming*, 171(1-2):115–166, 2018.

[10] Jerome Friedman, Trevor Hastie, and Robert Tibshirani. Sparse inverse covariance estimation with the graphical lasso. *Biostatistics*, 9(3):432–441, 12 2007.

[11] Dominique Guillot, Bala Rajaratnam, and Julien Emile-Geay. Statistical paleoclimate reconstructions via markov random fields. *Ann. Appl. Stat.*, 9(1):324–352, 03 2015.

[12] Cho-Jui Hsieh, Mátyás A. Sustik, Inderjit S. Dhillon, and Pradeep Ravikumar. Quic: Quadratic approximation for sparse inverse covariance estimation. *Journal of Machine Learning Research*, 15:2911–2947, 2014.

[13] Shuai Huang, Jing Li, Liang Sun, Jieping Ye, Adam Fleisher, Teresa Wu, Kewei Chen, and Eric Reiman. Learning brain connectivity of Alzheimer’s disease by sparse inverse covariance estimation. *NeuroImage*, 50(3):935 – 949, 2010.

[14] Keiiti Isii. On sharpness of tchebycheff-type inequalities. *Annals of the Institute of Statistical Mathematics*, 14(1):185–197, 1962.

[15] W. James and Charles Stein. Estimation with quadratic loss. In *Proceedings of the Fourth Berkeley Symposium on Mathematical Statistics and Probability, Volume 1: Contributions to the Theory of Statistics*, pages 361–379, Berkeley, Calif., 1961. University of California Press.

[16] Jana Jankova and Sara van de Geer. Inference in high-dimensional graphical models. 2018.

[17] Kshitij Khare, Sang-Yun Oh, and Bala Rajaratnam. A convex pseudolikelihood framework for high dimensional partial correlation estimation with convergence guarantees. *Journal of the Royal Statistical Society: Series B (Statistical Methodology)*, 77(4):803–825, sep 2015.

[18] Jan Krumsiek, Karsten Suhre, Thomas Illig, Jerzy Adamski, and Fabian J. Theis. Gaussian graphical modeling reconstructs pathway reactions from high-throughput metabolomics data. *BMC Systems Biology*, 5(1):21, Jan 2011.

[19] Clifford Lam and Jianqing Fan. Sparsity and rates of convergence in large covariance matrix estimation. *The Annals of Statistics*, 37(6B):4254–4278, 2009.

[20] Po-Ling Loh and Xin Lu Tan. High-dimensional robust precision matrix estimation: Cellwise corruption under ϵ -contamination. *Electron. J. Statist.*, 12(1):1429–1467, 2018.

[21] Rahul Mazumder and Trevor Hastie. Exact covariance thresholding into connected components for large-scale graphical lasso. *J. Mach. Learn. Res.*, 13(1):781–794, 2012.

[22] Patricia Menéndez, A. I. Yiannis Kourmpetis, Cajo J. F. ter Braak, and Fred A. van Eeuwijk. Gene regulatory networks from multifactorial perturbations using graphical lasso: Application to the dream4 challenge. *PLOS ONE*, 5(12):1–8, 12 2010.

[23] Viet Anh Nguyen, Daniel Kuhn, and Peyman Mohajerin Esfahani. Distributionally robust inverse covariance estimation: The Wasserstein shrinkage estimator. 2018.

[24] Jie Peng, Pei Wang, Nengfeng Zhou, and Ji Zhu. Partial correlation estimation by joint sparse regression models. *Journal of the American Statistical Association*, 104(486):735–746, 2009.

[25] David M.W. Powers. Evaluation: From precision, recall and f-factor to roc, informedness, markedness & correlation. *Journal of Machine Learning Technologies*, 2:37–63, 2011.

[26] Benjamin Rolfs, Bala Rajaratnam, Dominique Guillot, Ian Wong, and Arian Maleki. Iterative thresholding algorithm for sparse inverse covariance estimation. In F. Pereira, C. J. C. Burges, L. Bottou, and K. Q. Weinberger, editors, *Advances in Neural Information Processing Systems 25*, pages 1574–1582. Curran Associates, Inc., 2012.

[27] Adam J. Rothman, Peter J. Bickel, Elizaveta Levina, and Ji Zhu. Sparse permutation invariant covariance estimation. *Electron. J. Statist.*, 2:494–515, 2008.

[28] Soroosh Shafieezadeh-Abadeh, Peyman Mohajerin Esfahani, and Daniel Kuhn. Distributionally robust logistic regression. In *Advances in Neural Information Processing Systems 28*, pages 1576–1584. 2015.

[29] Stephen M. Smith, Karla L. Miller, Gholamreza Salimi-Khorshidi, Matthew Webster, Christian F. Beckmann, Thomas E. Nichols, Joseph D. Ramsey, and Mark W. Woolrich. Network modelling methods for fMRI. *NeuroImage*, 54(2):875 – 891, 2011.

[30] J. Michael Steele. *The Cauchy-Schwarz Master Class: An Introduction to the Art of Mathematical Inequalities*. Cambridge University Press, 2004.

[31] Nurgazy Sulaimanov, Sunil Kumar, Heinz Koepll, Frédéric Burdet, Marco Pagni, and Mark Ibberson. Inferring gene expression networks with hubs using a degree weighted Lasso approach. *Bioinformatics*, 35(6):987–994, 08 2018.

[32] Joong-Ho Won, Johan Lim, Seung-Jean Kim, and Bala Rajaratnam. Condition-number-regularized covariance estimation. *Journal of the Royal Statistical Society: Series B (Statistical Methodology)*, 75(3):427–450, dec 2012.

[33] Lingzhou Xue and Hui Zou. Regularized rank-based estimation of high-dimensional paranormal graphical models. *The Annals of Statistics*, 40(5):2541–2571, 2012.

[34] Eunho Yang and Aurelie C Lozano. Robust Gaussian graphical modeling with the trimmed graphical lasso. In *Advances in Neural Information Processing Systems 28*, pages 2602–2610. 2015.

[35] Sen Yang, Qian Sun, Shuiwang Ji, Peter Wonka, Ian Davidson, and Jieping Ye. Structural graphical lasso for learning mouse brain connectivity. In *Proceedings of the 21th ACM SIGKDD International Conference on Knowledge Discovery and Data Mining*. ACM, 2015.

[36] Ming Yuan and Yi Lin. Model selection and estimation in the Gaussian graphical model. *Biometrika*, 94(1):19–35, 2007.

A Proofs for the paper

A.1 Proof of Theorem 2.1

Proof. Consider $K \in \mathbb{S}_d^{++}$. Observe that the function $l(\cdot; K) : \mathbb{S}_d \rightarrow \mathbb{R}$ is Borel measurable since it is a continuous function. Then, we use the duality result for the DRO formulation from Proposition B.2 from the appendix of this paper and obtain

$$\sup_{P: \mathcal{D}_c(P, \mathbb{P}_n) \leq \delta} E_P[l(W; K)] = \inf_{\gamma \geq 0} \left\{ \gamma \delta + \frac{1}{n} \sum_{i=1}^n \left(\sup_{W \in \mathbb{S}_d} \{l(W; K) - \gamma c(W, W_i)\} \right) \right\}. \quad (19)$$

Let $\Delta := W - W_i$. Then,

$$\begin{aligned} & \sup_{W \in \mathbb{S}_d} \{l(W; K) - \gamma c(W, W_i)\} \\ &= \sup_{W \in \mathbb{S}_d} \{\text{trace}(KW) - \log |K| - \gamma \|\text{vec}(W) - \text{vec}(W_i)\|_q^\rho\} \\ &= \sup_{\Delta \in \mathbb{S}_d} \{\text{trace}(K(\Delta + W_i)) - \gamma \|\text{vec}(\Delta)\|_q^\rho\} - \log |K| \\ &= \sup_{\Delta \in \mathbb{S}_d} \{\text{trace}(K\Delta) - \gamma \|\text{vec}(\Delta)\|_q^\rho\} + \text{trace}(KW_i) - \log |K| \\ &= \sup_{\Delta \in \mathcal{M}(K)} \{\|\text{vec}(\Delta)\|_q \|\text{vec}(K)\|_p - \gamma \|\text{vec}(\Delta)\|_q^\rho\} + \text{trace}(KW_i) - \log |K| \end{aligned} \quad (20)$$

with $\mathcal{M}(K) = \{\Delta \in \mathbb{S}_d \mid \text{trace}(K\Delta) > 0, |\Delta_{ij}|^q = \theta |k_{ij}|^p \text{ for some } \theta > 0\}$ so that the fourth line follows from selecting a $\Delta \in \mathbb{S}_d$ (since $K \in \mathbb{S}_d^{++}$) such that Holder's inequality holds tightly (with $\frac{1}{p} + \frac{1}{q} = 1$). In fact, Holder's inequality holds tightly if and only if $\Delta \in \mathcal{M}(K)$ [30, Chapter 9], even for the limiting case $q = \infty, p = 1$. Observe that there exist multiple $\Delta \in \mathbb{S}_d$ that can satisfy Holder's inequality tightly. As a consequence, we are still free to choose the magnitude of the q -norm of such $\text{vec}(\Delta)$ (and this is what we will use next).

Now, the argument inside the supremum in the last line of (20) is a polynomial function on $\|\text{vec}(\Delta)\|_q$. We have to analyze two cases.

Case 1: $\rho = 1$. In this case we observe that, by setting $\epsilon(\gamma, K) = \sup_{\Delta \in \mathcal{M}(K)} \{\|\text{vec}(\Delta)\|_q (\|\text{vec}(K)\|_p - \gamma)\}$:

- if $\gamma \geq \|\text{vec}(K)\|_p$, then $\epsilon(\gamma, K) = 0$ (in particular, if $\gamma = \|\text{vec}(K)\|_p$, the optimizer is $\Delta = \mathbb{0}_{d \times d}$);
- if $\gamma < \|\text{vec}(K)\|_p$, then $\epsilon(\gamma, K) = \infty$;

so that, recalling (19), due to the outside infimum to be taken over $\gamma \geq 0$; and so we must have that

$$\sup_{P: \mathcal{D}_c(P, \mathbb{P}_n) \leq \delta} E_P[l(W; K)] = \inf_{\gamma \geq \|\text{vec}(K)\|_p} \left\{ \gamma \delta + \frac{1}{n} \sum_{i=1}^n (\text{trace}(KW_i) - \log |K|) \right\}$$

from which we immediately obtain (8).

Case 2: $\rho > 1$. By differentiation and basic calculus (e.g., using the first and second derivative test) we obtain that the maximizer

$$\Delta^* = \arg \sup_{\Delta \in \mathcal{M}(K)} \{\|\text{vec}(\Delta)\|_q \|\text{vec}(K)\|_p - \gamma \|\text{vec}(\Delta)\|_q^\rho\}$$

is such that $\|\text{vec}(\Delta^*)\|_q = \left(\frac{\|\text{vec}(K)\|_p}{\gamma \rho}\right)^{\frac{1}{\rho-1}}$. Then,

$$\begin{aligned} \sup_{W \in \mathbb{S}_d} \{l(W; K) - \gamma c(W, W_i)\} &= \frac{\|\text{vec}(K)\|_p^{\frac{\rho}{\rho-1}}}{(\gamma \rho)^{\frac{1}{\rho-1}}} - \gamma \left(\frac{\|\text{vec}(K)\|_p}{\gamma \rho}\right)^{\frac{\rho}{\rho-1}} + \text{trace}(KW_i) \\ &\quad - \log |K| \\ &= \|\text{vec}(K)\|_p^{\frac{\rho}{\rho-1}} \frac{\rho-1}{\rho^{\frac{\rho}{\rho-1}} \gamma^{\frac{1}{\rho-1}}} + \text{trace}(KW_i) - \log |K|. \end{aligned} \quad (21)$$

Replacing this back in (19),

$$\begin{aligned}
& \sup_{P: \mathcal{D}_c(P, \mathbb{P}_n) \leq \delta} E_P[l(W; K)] \\
&= \inf_{\gamma \geq 0} \left\{ \gamma \delta + \frac{1}{n} \sum_{i=1}^n \left(\|\mathbf{vec}(K)\|_p^{\frac{\rho}{\rho-1}} \frac{\rho-1}{\rho^{\frac{\rho}{\rho-1}} \gamma^{\frac{1}{\rho-1}}} + \text{trace}(KW_i) - \log |K| \right) \right\} \\
&= \inf_{\gamma \geq 0} \left\{ \gamma \delta + \|\mathbf{vec}(K)\|_p^{\frac{\rho}{\rho-1}} \frac{\rho-1}{\rho^{\frac{\rho}{\rho-1}} \gamma^{\frac{1}{\rho-1}}} + \text{trace} \left(K \frac{1}{n} \sum_{i=1}^n W_i \right) - \log |K| \right\} \\
&= \inf_{\gamma \geq 0} \left\{ \gamma \delta + \|\mathbf{vec}(K)\|_p^{\frac{\rho}{\rho-1}} \frac{\rho-1}{\rho^{\frac{\rho}{\rho-1}} \gamma^{\frac{1}{\rho-1}}} \right\} + \text{trace}(KA_n) - \log |K|. \tag{22}
\end{aligned}$$

Now, we observe that the argument inside the infimum in the last line of (22) is a function that grows to infinity when $\gamma \rightarrow 0$ or $\gamma \rightarrow \infty$, so that the minimum is attained for some optimal γ . By using the first and second derivative tests, we obtain that the minimizer is $\gamma^* = \frac{\|\mathbf{vec}(K)\|_p}{\rho \delta^{\frac{\rho-1}{\rho}}}$. Then, replacing this back in (22) and then this in (19), we finally obtain (8) after some algebraic simplification. \square

A.2 Proof of Lemma 3.1

Proof. Consider $K \in \mathbb{S}_d^{++}$ and define $g(K) = \sup_{P: \mathcal{D}_c(P, \mathbb{P}_n) \leq \delta} E_P[l(W; K)]$ for a fixed δ . We prove (12), by a direct application of Proposition 8 of [2, Appendix C], observing that we satisfy the three conditions for its application:

- (i) g is convex on \mathbb{S}_d^{++} and finite,
- (ii) there exists $b \in \mathbb{R}$ such that the sublevel set $\kappa_b = \{K \mid g(K) \leq b\}$ is compact and non-empty,
- (iii) $E_P[l(W; K)]$ is lower semi-continuous and convex as a function of K throughout κ_b for any $P \in \{P \mid \mathcal{D}_c(P, \mathbb{P}_n) \leq \delta\}$.

First, we observe that

$$E_{\mathbb{P}_0}[l(W, K)] = E_{\mathbb{P}_0}[\text{trace}(KW) - \log |K|] \leq \text{trace}(KE_{\mathbb{P}_0}[W]) < \infty,$$

since $E_{\mathbb{Q}_0}(\|X\|_2^2) < \infty$. Then, using Theorem 2.1, the function

$$g(K) = \sup_{P: \mathcal{D}_c(P, \mathbb{P}_n) \leq \delta} E_P[l(W; K)] = \text{trace}(KA_n) - \log |K| + \delta^{1/\rho} \|\mathbf{vec}(K)\|_p$$

is finite. Moreover, we also claim it is convex for all $K \in \mathbb{S}_d^{++}$. This follows from the fact that $\text{trace}(KA_n) - \log |K|$ and $\|\mathbf{vec}(K)\|_p$, $p \in [1, \infty]$ are two convex functions on $K \in \mathbb{S}_d^{++}$, and from the fact that the nonnegative weighted sum of two convex functions is another convex function [5]. This proves (i).

Now, we claim that $g(K)$ is radially unbounded, i.e., $g(K) \rightarrow \infty$ as $\|\mathbf{vec}(K)\|_p \rightarrow \infty$. To see this, recall that $\text{trace}(KA_n) - \log |K|$ is a differentiable convex function in K that is minimized whenever $K^{-1} = A_n$, since A_n is invertible for $n > d$ almost surely. Then,

$$g(K) = \text{trace}(KA_n) - \log |K| + \delta^{1/\rho} \|\mathbf{vec}(K)\|_p \geq d - \log |A_n^{-1}| + \delta^{1/\rho} \|\mathbf{vec}(K)\|_p,$$

from which it immediately follows that $g(K) \rightarrow \infty$ as $\|\mathbf{vec}(K)\|_p \rightarrow \infty$.

Now, again, since $g(K)$ is also convex and continuous in \mathbb{S}_d^{++} , we conclude that the level sets $\kappa_b = \{K \mid g(K) \leq b\}$ are compact and nonempty as long as $b > l(W; K) + \delta^{1/\rho} \|\mathbf{vec}(K)\|_p$. This proves (ii). Moreover, since $l(W; K)$ is convex and continuous on any $K \in \mathbb{S}_d^{++}$, it follows that $E_P[l(W; K)]$ for any $P \in \{P \mid \mathcal{D}_c(P, \mathbb{P}_n) \leq \delta\}$ is also continuous and convex on any $K \in \mathbb{S}_d^{++}$, thus (iii) follows immediately. \square

A.3 Proof of Theorem 3.2

Proof. Consider $K \in \mathbb{S}_d^{++}$. Setting $h(U; K) = U - K^{-1}$, it is clear that we satisfy the conditions for applying Proposition B.1 in the Appendix, and so we obtain

$$R_n(K) = \sup_{\Lambda \in \mathbb{S}_d} \left\{ -\frac{1}{n} \sum_{i=1}^n \sup_{U \in \mathbb{S}_d} \{ \text{trace}(\Lambda^\top (U - K^{-1})) - \|\mathbf{vec}(U) - \mathbf{vec}(W_i)\|_q^\rho \} \right\} \tag{23}$$

Now, letting $\Delta := U - W_i^\top$

$$\begin{aligned}
& \sup_{U \in \mathbb{S}_d} \{ \text{trace}(\Lambda^\top(U - K^{-1})) - \|\text{vec}(U) - \text{vec}(W_i)\|_q^\rho \} \\
&= \sup_{\Delta \in \mathbb{S}_d} \{ \text{trace}(\Lambda^\top(\Delta + W_i - K^{-1})) - \|\text{vec}(\Delta)\|_q^\rho \} \\
&= \sup_{\Delta \in \mathbb{S}_d} \{ \text{trace}(\Lambda^\top \Delta) - \|\text{vec}(\Delta)\|_q^\rho \} + \text{trace}(\Lambda^\top(W_i - K^{-1})) \quad (24) \\
&= \sup_{\Delta \in \mathcal{M}(\Lambda)} \{ \|\text{vec}(\Lambda)\|_p \|\text{vec}(\Delta)\|_q - \|\text{vec}(\Delta)\|_q^\rho \} \\
&\quad + \text{trace}(\Lambda^\top(W_i - K^{-1}))
\end{aligned}$$

with $\mathcal{M}(\Lambda)$ as in the proof of Theorem 2.1, so that the third line follows from selecting a $\Delta \in \mathbb{S}_d$ such that Holder's inequality holds tightly (with $\frac{1}{p} + \frac{1}{q} = 1$), whose existence has been explained in the proof of Theorem 2.1. Thus, we are still free to choose the magnitude of the q -norm of such $\text{vec}(\Delta)$ (and this is what we will use next).

Now, the argument inside the supremum in the last line of (24) is a polynomial function on $\|\text{vec}(\Delta)\|_q$. We have to analyze two cases.

Case 1: $\rho = 1$. In this case we observe that, by setting $\epsilon(\Lambda) = \sup_{\Delta \in \mathbb{S}_d} \{ \|\text{vec}(\Delta)\|_q (\|\text{vec}(\Lambda)\|_p - 1) \}$:

- if $\|\text{vec}(\Lambda)\|_p \leq 1$, then $\epsilon(\Lambda) = 0$ (in particular, if $\|\text{vec}(\Lambda)\|_p < 1$, the optimizer is $\Delta = \mathbb{0}_{d \times d}$);
- if $\|\text{vec}(\Lambda)\|_p > 1$, then $\epsilon(\Lambda) = \infty$;

so that, recalling (23), we see that if $\|\text{vec}(\Lambda)\|_p > 1$, then $R_n(K) = -\infty$. Then, we obtain that

$$\begin{aligned}
R_n(K) &= \sup_{\Lambda \in \mathbb{S}_d: \|\text{vec}(\Lambda)\|_p \leq 1} \left\{ -\frac{1}{n} \sum_{i=1}^n \text{trace}(\Lambda^\top(W_i - K^{-1})) \right\} \\
&= \sup_{\Lambda \in \mathbb{S}_d: \|\text{vec}(\Lambda)\|_p \leq 1} \{ -\text{trace}(\Lambda^\top(A_n - K^{-1})) \} \\
&= \sup_{\Lambda \in \mathbb{S}_d: \|\text{vec}(\Lambda)\|_p \leq 1} \{ \text{vec}(\Lambda)^\top \text{vec}(A_n - K^{-1}) \} \\
&= \|\text{vec}(A_n - K^{-1})\|_q
\end{aligned}$$

where the third line results from the fact that Λ is a free variable so we can flip its sign, and the last line follows from the the analysis of conjugate norms and the fact that $\Lambda, A_n - K^{-1} \in \mathbb{S}_d$. We thus obtained (16).

Case 2: $\rho > 1$. By differentiation and basic calculus (e.g., using the first and second derivative test) we obtain that the maximizer

$$\Delta^* = \arg \sup_{\Delta \in \mathbb{S}_d} \{ \|\text{vec}(\Delta)\|_q \|\text{vec}(\Lambda)\|_p - \gamma \|\text{vec}(\Delta)\|_q^\rho \}$$

is such that $\|\text{vec}(\Delta^*)\|_q = \left(\frac{\|\text{vec}(K)\|_p}{\rho} \right)^{\frac{1}{\rho-1}}$. Then, replacing this back in (23),

$$\begin{aligned}
R_n(K) &= \sup_{\Lambda \in \mathbb{S}_d} \left\{ -\frac{1}{n} \sum_{i=1}^n \left(\|\text{vec}(\Lambda)\|_p^{\frac{\rho}{\rho-1}} \frac{\rho-1}{\rho^{\frac{\rho}{\rho-1}}} + \text{trace}(\Lambda^\top(W_i - K^{-1})) \right) \right\} \\
&= \sup_{\Lambda \in \mathbb{S}_d} \left\{ -\|\text{vec}(\Lambda)\|_p^{\frac{\rho}{\rho-1}} \frac{\rho-1}{\rho^{\frac{\rho}{\rho-1}}} - \text{trace}(\Lambda^\top(A_n - K^{-1})) \right\} \\
&= \sup_{\Lambda \in \mathbb{S}_d} \left\{ \text{trace}(\Lambda^\top(A_n - K^{-1})) - \|\text{vec}(\Lambda)\|_p^{\frac{\rho}{\rho-1}} \frac{\rho-1}{\rho^{\frac{\rho}{\rho-1}}} \right\} \\
&= \sup_{\Lambda \in \mathbb{S}_d} \left\{ \|\text{vec}(\Lambda)\|_p \|\text{vec}(A_n - K^{-1})\|_q - \|\text{vec}(\Lambda)\|_p^{\frac{\rho}{\rho-1}} \frac{\rho-1}{\rho^{\frac{\rho}{\rho-1}}} \right\}.
\end{aligned}$$

Again, by differentiation and basic calculus, we obtain that the maximizer Λ^* is such that $\|\text{vec}(\Lambda^*)\|_p = \rho \|\text{vec}(A_n - K^{-1})\|_q^{\rho-1}$. Replacing this value back in our previous expression, we get that $R_n(K) = \|\text{vec}(A_n - K^{-1})\|_q^\rho$, and thus we showed (16). \square

B Applicability of the dual representations of the RWP function and the DRO formulation

The dual representations of the RWP function and the DRO formulation for the case in which the space of probability measures is $\mathcal{P}(\mathbb{R}^d \times \mathbb{R}^d)$ is studied in the paper [2]. In this paper, we are interested in the case $\mathcal{P}(\mathbb{S}_d \times \mathbb{S}_d)$. In other words, we consider the samples to be in \mathbb{S}_d instead of \mathbb{R}^d . We want to emphasize that the derivations of these dual representations rely on the dual formulation of the so called “problem of moments” or a specific class of “Chebyshev-type inequalities” referenced in the work by Isii [14]. The derivation by Isii is actually more general in the sense that is applied to more general probability spaces than the ones used in this paper and in [2] (in fact, it is stated for general spaces of non-negative measures).

Throughout this section, we consider an integrable function $h : \mathbb{S}_d \times \mathbb{S}_d \rightarrow \mathbb{S}_d$, and a lower semi-continuous function $c : \mathbb{S}_d \times \mathbb{S}_d \rightarrow [0, \infty)$ such that $c(U, U) = 0$ for any $U \in \mathbb{S}_d$ and such that the set

$$\Omega := \{(U', W') \in \mathbb{S}_d \times \mathbb{S}_d \mid c(U', W') < \infty\}$$

is Borel measurable and non-empty. Also consider an iid random sample $W_1, \dots, W_n \sim W$ with W coming from a distribution on $\mathcal{P}(\mathbb{S}_d)$.

Now, let us focus first on the RWP function in the following proposition which parallels [2, Proposition 3].

Proposition B.1. *Consider $K \in \mathbb{S}_d^{++}$. Let $h(\cdot, K)$ be Borel measurable. Also, suppose that $\mathbb{O}_{d \times d}$ lies in the interior of the convex hull of $\{h(U', K) \mid U' \in \mathbb{S}_d\}$. Then,*

$$R_n(K) = \sup_{\Lambda \in \mathbb{S}_d} \left\{ -\frac{1}{n} \sum_{i=1}^n \sup_{U \in \mathbb{S}_d} \{\text{trace}(\Lambda^\top h(U; K)) - c(U, W_i)\} \right\}.$$

Proof. Consider the proof of [2, Proposition 3]. If we:

- set the estimating equation by $E[h(W; K)] = \mathbb{O}_{d \times d}$,
- set

$$R_n(K) = \inf \{E_\pi[c(U, W)] \mid E_\pi[h(U; K)] = \mathbb{O}_{n \times n}, \pi_W = \mathbb{P}_n, \pi \in \mathcal{P}(\mathbb{S}_d \times \mathbb{S}_d)\},$$

with π_W denoting the marginal distribution of W ,

- consider the previously defined Ω ,

then we obtain that, following the rest of this proof (and using [14, Theorem 1] with its special case):

$$\begin{aligned} R_n(K) &= \sup_{\Lambda \in \mathbb{S}_d} \left\{ -\frac{1}{n} \sum_{i=1}^n \sup_{U \in \mathbb{S}_d} \{\text{vec}(\Lambda)^\top \text{vec}(h(U; K)) - c(U, W_i)\} \right\} \\ &= \sup_{\Lambda \in \mathbb{S}_d} \left\{ -\frac{1}{n} \sum_{i=1}^n \sup_{U \in \mathbb{S}_d} \{\text{trace}(\Lambda^\top h(U; K)) - c(U, W_i)\} \right\}, \end{aligned}$$

thus obtaining the dual representation of the RWP function. \square

The following proposition for the dual representation of the DRO formulation parallels [2, Proposition 1].

Proposition B.2. *For $\gamma \geq 0$ and loss functions $l(U'; K)$ that are upper semi-continuous in $U' \in \mathbb{S}_d$ for each $K \in \mathbb{S}_d^{++}$, let*

$$\phi_\gamma(W_i; K) = \sup_{U \in \mathbb{S}_d} \{l(U; K) - \gamma c(U, W_i)\}. \quad (25)$$

Then

$$\sup_{P: \mathcal{D}_c(P, \mathbb{P}_n) \leq \delta} E_P[l(W; K)] = \min_{\gamma \geq 0} \left\{ \gamma \delta + \frac{1}{n} \sum_{i=1}^n \phi_\gamma(W_i; K) \right\}.$$

Proof. The proof for the dual representation of the DRO for our domain of symmetric matrices is also very similar to the one described in Proposition 4 of [2, version 2], just by following appropriate similar changes as we did for the proof of B.1. \square

C Figures, tables and additional analysis for the numerical results (Section 4 of the paper)

C.1 Matthews correlation coefficient analysis

Let true positives (TP) be the number of nonzero off-diagonal entries of Ω that are correctly identified, false negatives (FN) be the number of its nonzero off-diagonal entries that are incorrectly identified as zeros, false positives (FP) be the number of its zero off-diagonal entries that are incorrectly identified as nonzeros, and true negatives (TN) be the number of its zero off-diagonal entries that are correctly identified. Given the estimated precision matrix \hat{K} , the Matthews correlation coefficient (MCC) [25] is defined as:

$$MCC = \frac{TP \cdot TN - FP \cdot FN}{\sqrt{(TP + FP)(TP + FN)(TN + FP)(TN + FN)}}, \quad (26)$$

and, whenever the denominator is zero, it can be arbitrarily set to one. It can be shown that $MCC \in [-1, +1]$, and $+1$ is interpreted as a perfect prediction (of both zero and nonzero values), 0 is interpreted as prediction no better than a random one, and -1 is interpreted as indicating total disagreement between prediction and observation.

MCC has been argued to be one of the most informative coefficients for assessing the performance of binary classification (in this case, classifying if an entry of the precision matrix is zero or nonzero) since it summarizes all information from the TP, TN, FP and FN quantities [7, 25], in contrast to other measures like TPR and FPR.

		RS				CV	
		α					
		0.21	0.56	0.79	0.90		
n	50	0	27.5e-2 (1.2)	79.0e-2 (1.8)	1.3 (2.1)	3.7 (1.4)	
	75	41.8e-3 (41.7e-2)	32.3e-2 (1.2)	1.2 (2.1)	1.9 (2.2)	6.0 (1.7)	
	200	39.0e-2 (1.2)	2.1 (2.6)	3.8 (2.7)	5.2 (2.6)	14.8 (2.0)	
	600	7.0 (2.6)	12.4 (2.3)	15.8 (2.1)	18.7 (2.0)	34.3 (1.7)	
	1000	15.7 (2.2)	23.2 (2.1)	27.8 (1.9)	30.8 (2.0)	41.9 (1.7)	
	2500	44.5 (1.9)	53.8 (1.7)	59.0 (1.7)	62.1 (1.6)	48.4 (1.5)	
	10000	92.3 (76.5e-2)	94.9 (61.8e-2)	96.0 (53.4e-2)	96.4 (54.8e-2)	49.0 (1.6)	

Table 1: Average values for the MCC (along with its standard deviations) over $N = 200$ datasets for the selection of the regularization parameter under the RobSel algorithm (RS) (under different parameter values α) and cross-validation (CV). All entries of the table are multiplied by 100. We have highlighted with a bold font those combinations of parameter values α and sample size n in which RS gives a comparable or even better performance than CV.

C.2 Regularization parameters

All the plots related to the RS and BN criteria for choosing λ have in their x-axis the values $\alpha \in \{0.10, 0.21, 0.33, 0.44, 0.56, 0.67, 0.79, 0.90\}$. We study the cases for sample sizes $n \in \{50, 75, 120, 200, 600, 1000, 10000\}$.

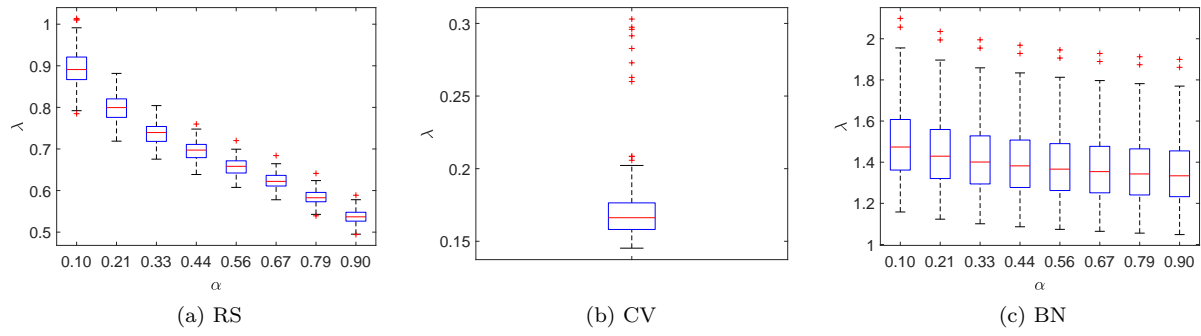


Figure 2: $n = 50$

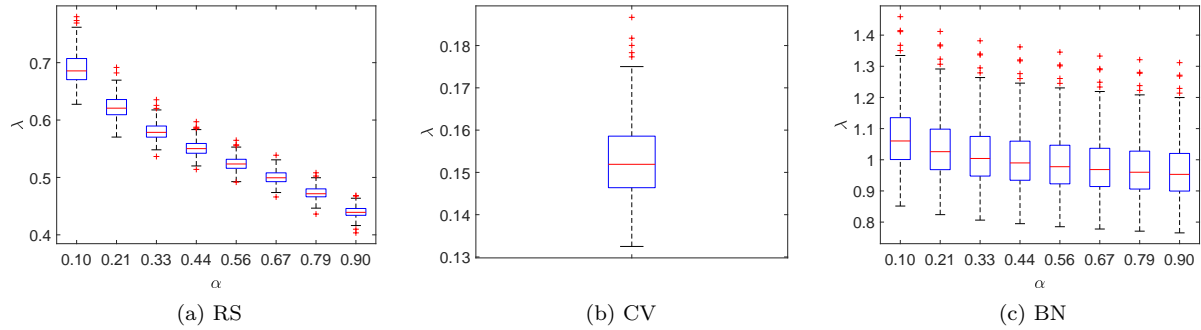


Figure 3: $n = 75$

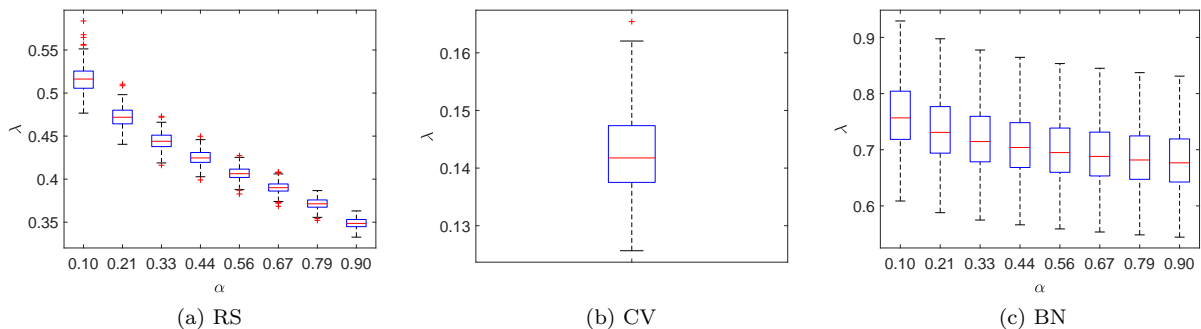


Figure 4: $n = 120$

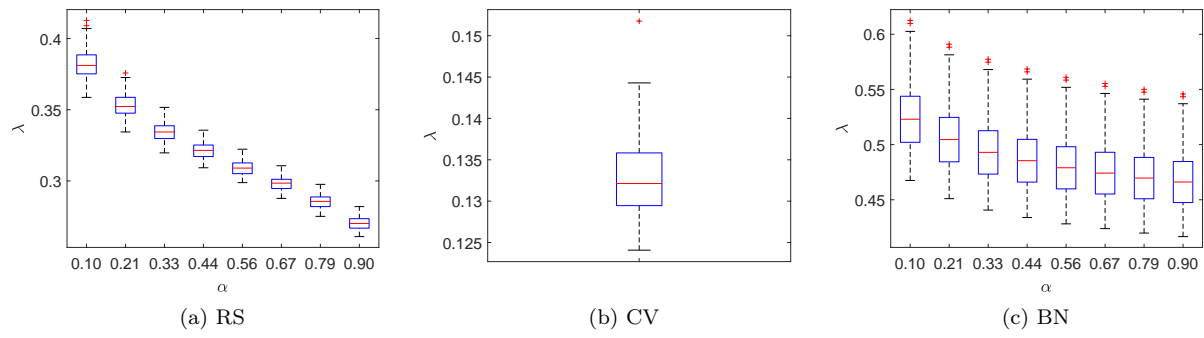


Figure 5: $n = 200$

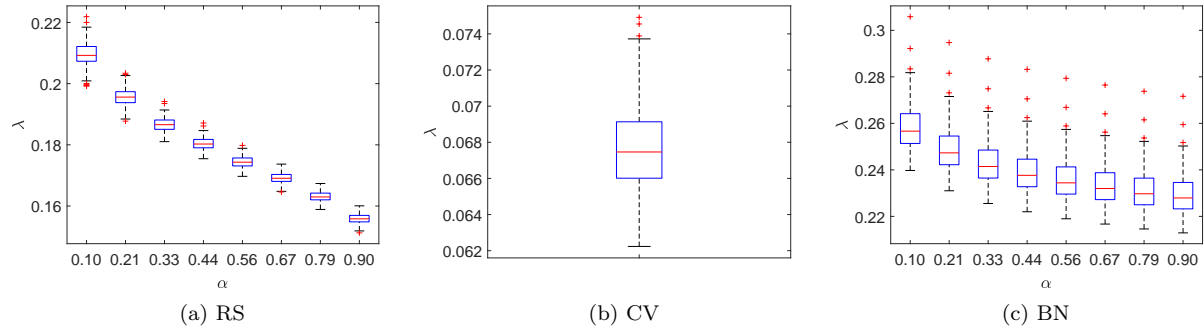


Figure 6: $n = 600$

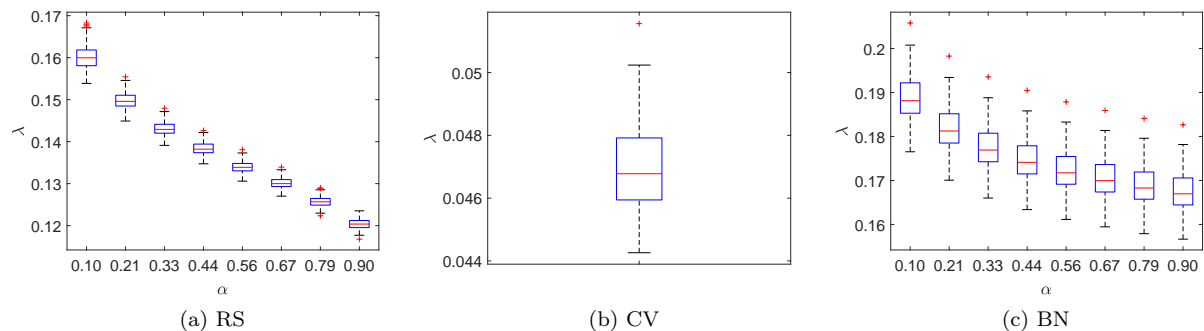


Figure 7: $n = 1000$

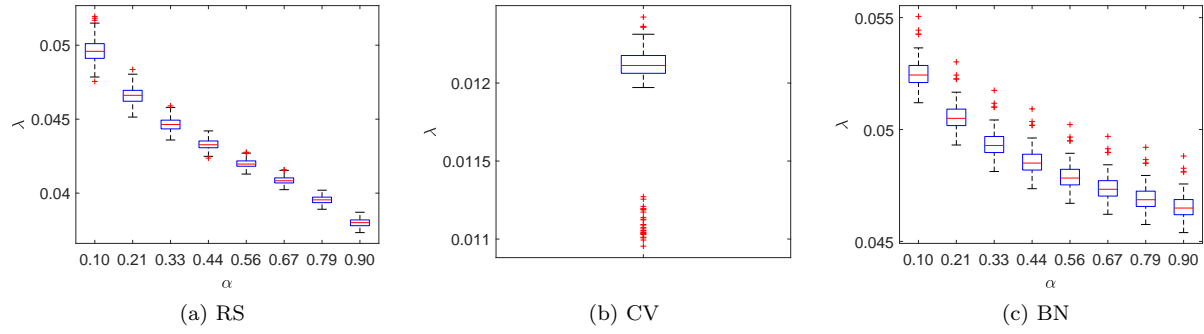


Figure 8: $n = 10000$

C.3 Performance figures for different choices of the regularization parameter

All the plots related to the RS, BN and RWP criteria for choosing λ have in their x-axis the values $\alpha \in \{0.10, 0.21, 0.33, 0.44, 0.56, 0.67, 0.79, 0.90\}$. We study the cases for sample sizes $n \in \{50, 75, 120, 200, 600, 1000, 10000\}$.

C.3.1 $n = 50$

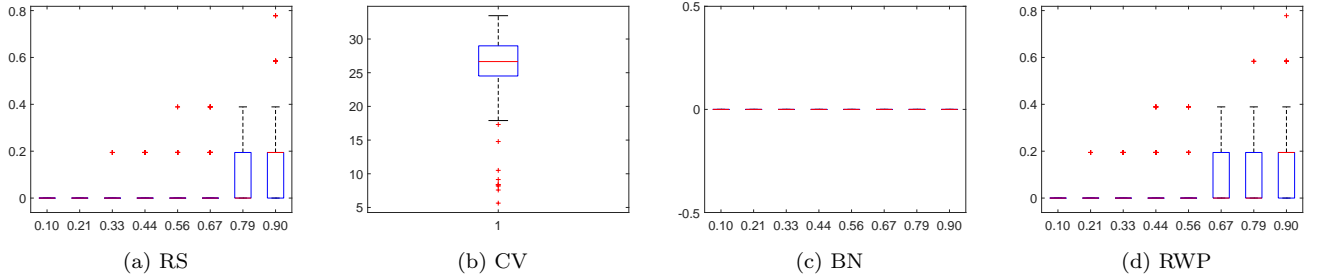


Figure 9: True positive rate (%)

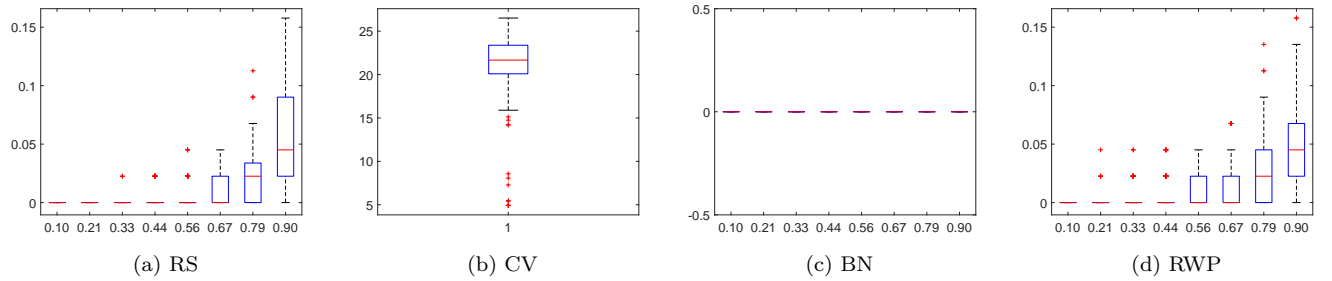


Figure 10: False positive rate (%)

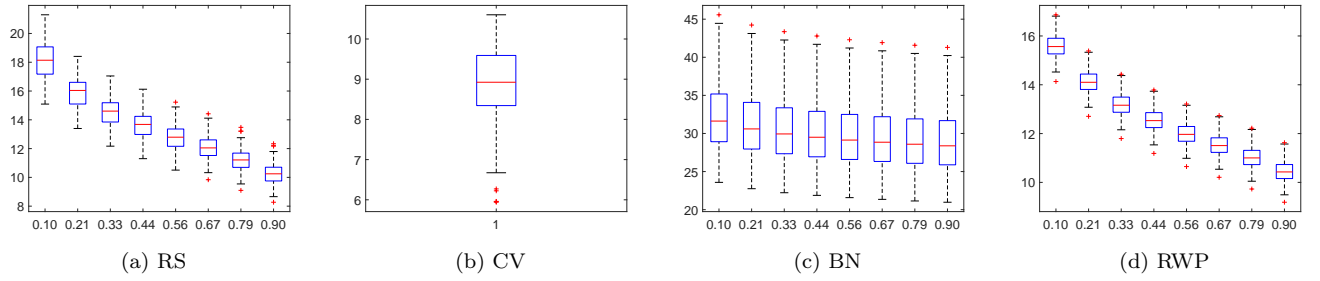


Figure 11: Stein's loss

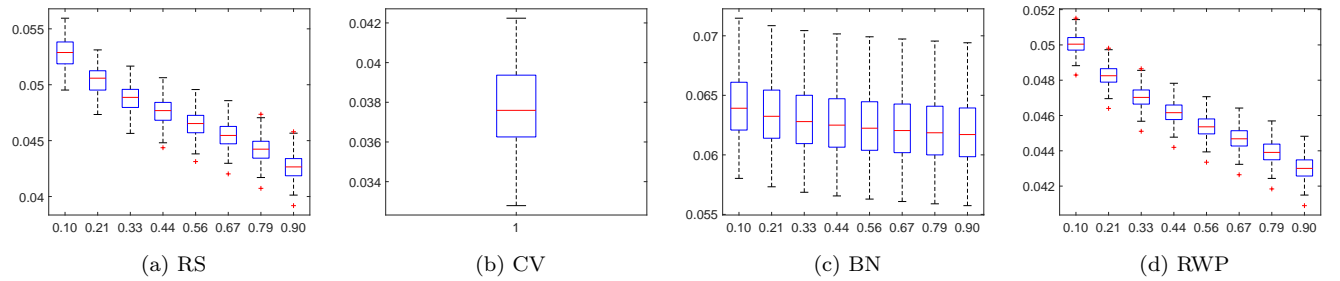


Figure 12: Norm of difference of (inverse) covariances

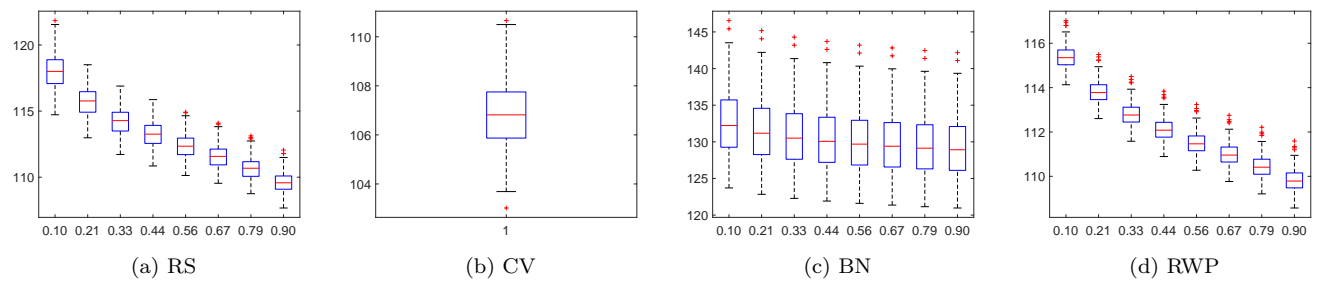


Figure 13: Out of sample loss

C.3.2 $n = 75$

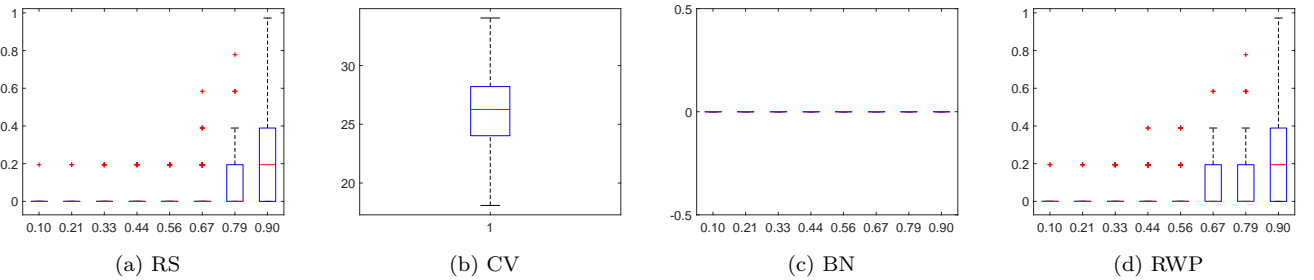


Figure 14: True positive rate (%)

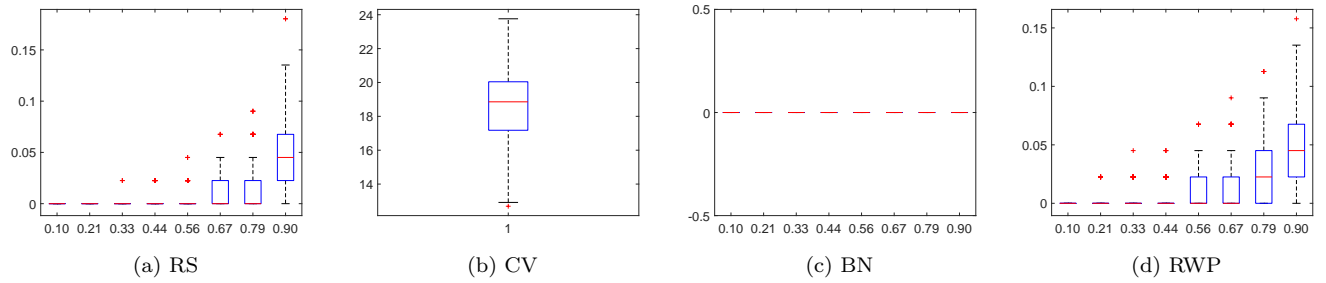


Figure 15: False positive rate (%)

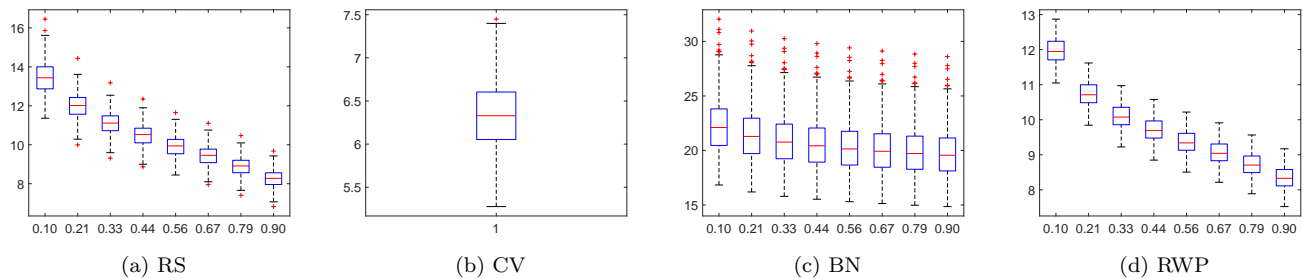


Figure 16: Stein's loss

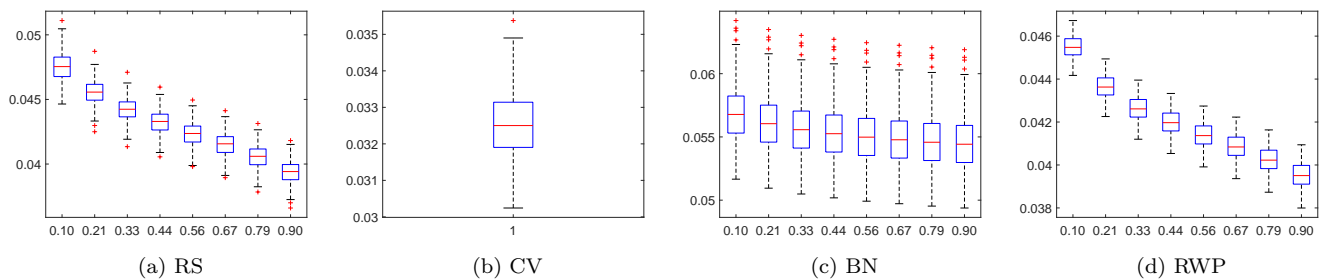


Figure 17: Norm of difference of (inverse) covariances

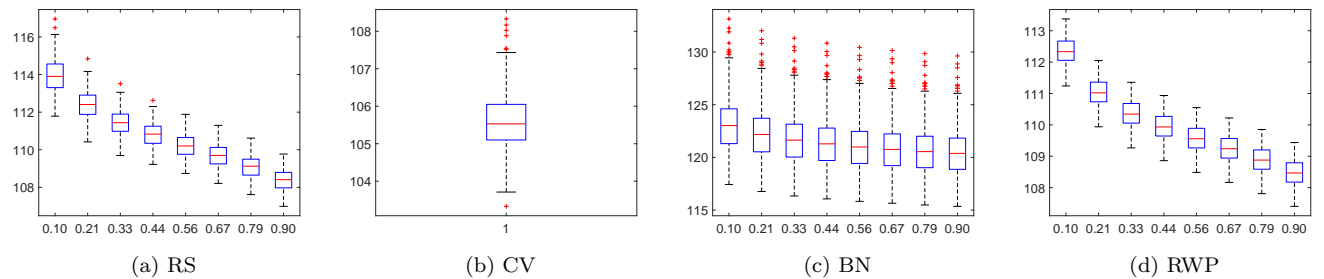


Figure 18: Out of sample loss

C.3.3 $n = 120$

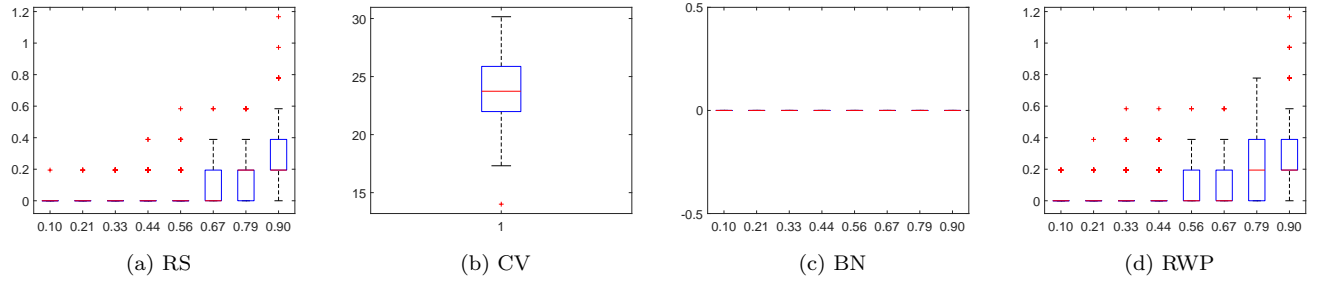


Figure 19: True positive rate (%)

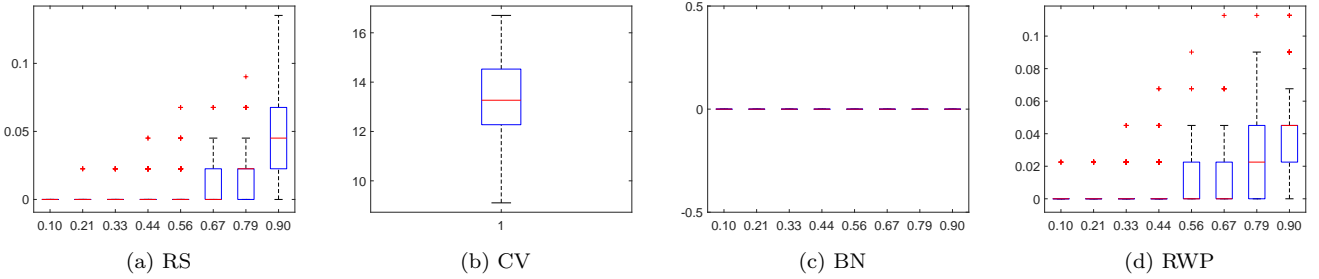


Figure 20: False positive rate (%)

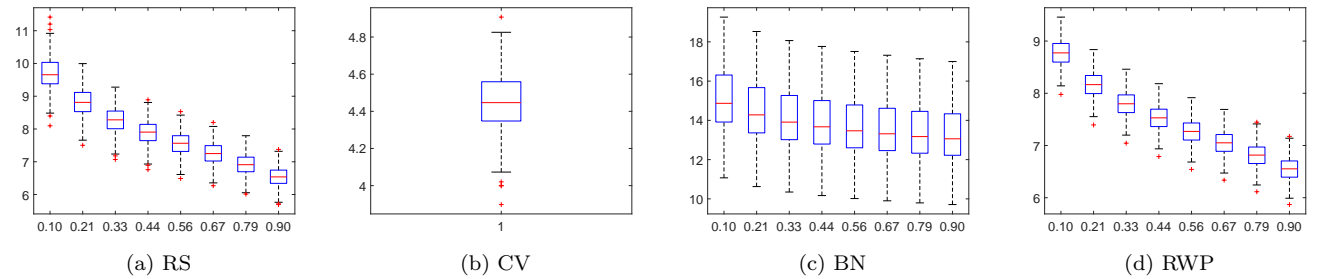


Figure 21: Stein's loss

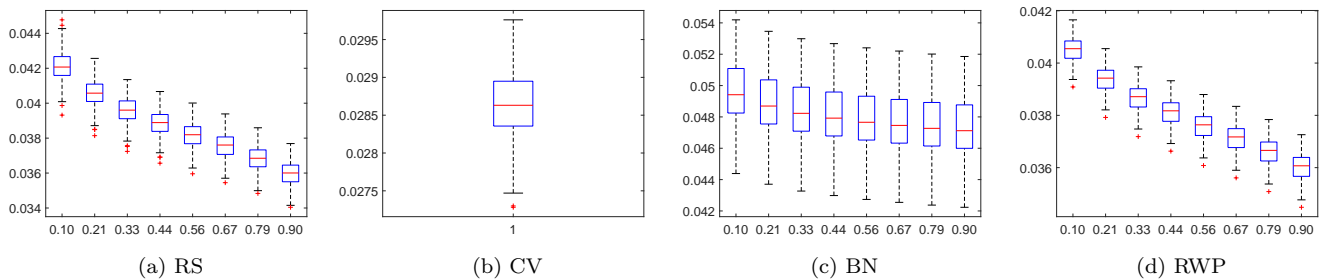


Figure 22: Norm of difference of (inverse) covariances

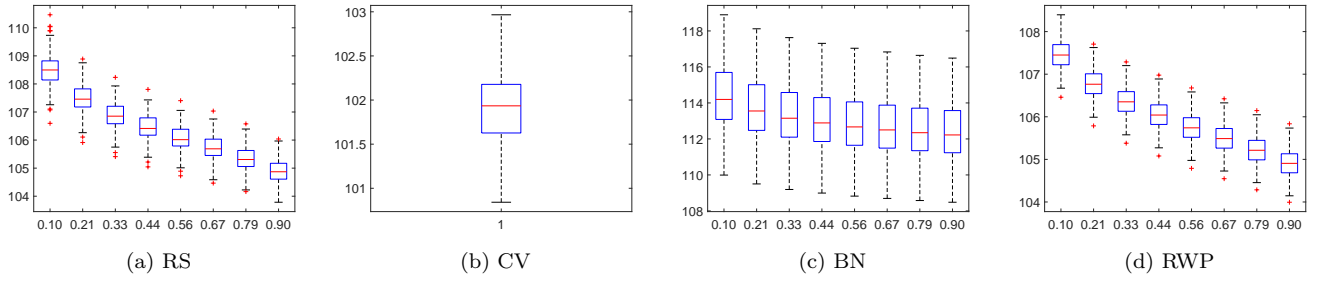


Figure 23: Out of sample loss

C.3.4 $n = 200$

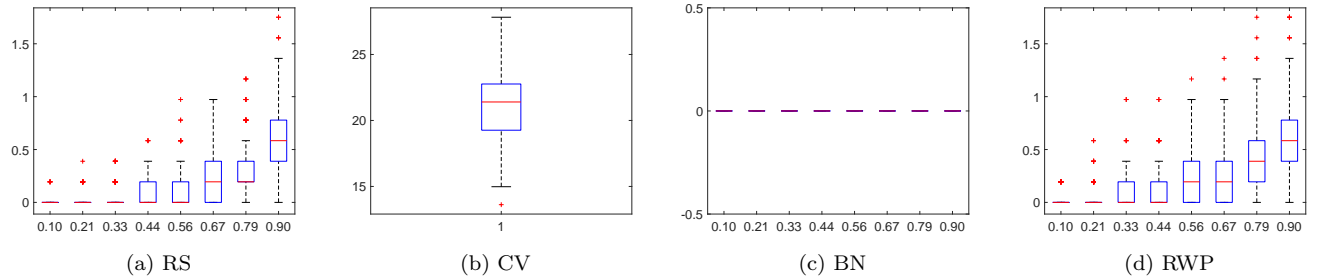


Figure 24: True positive rate (%)

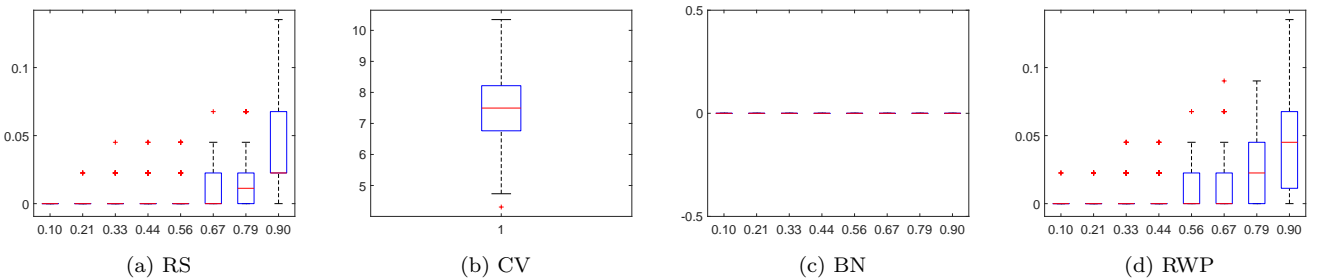


Figure 25: False positive rate (%)

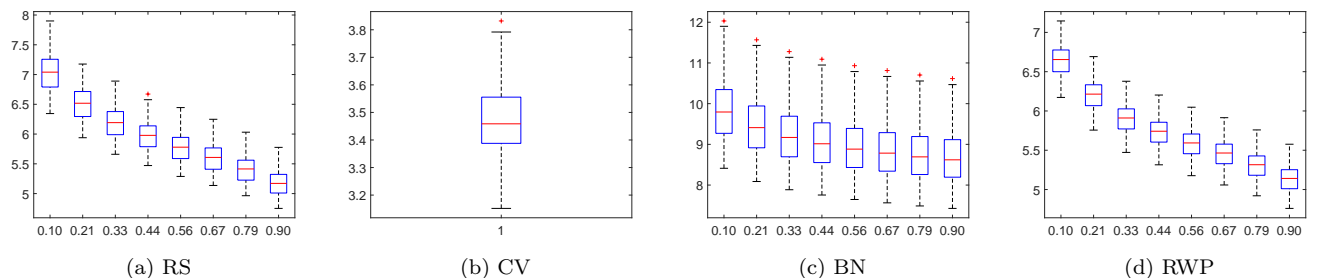


Figure 26: Stein's loss

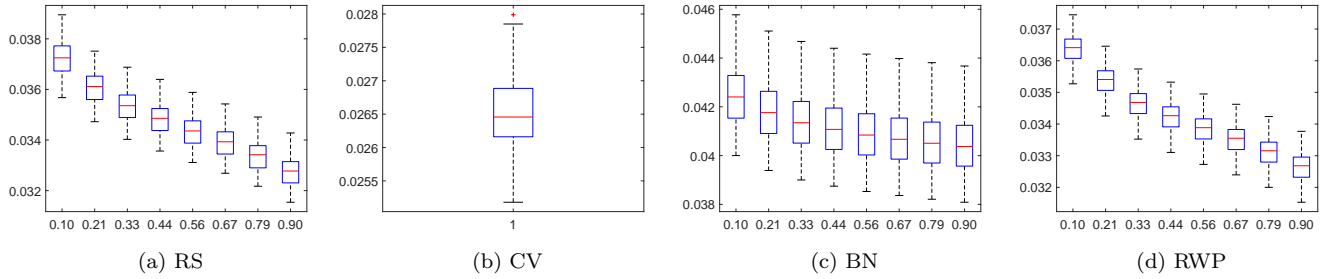


Figure 27: Norm of difference of (inverse) covariances

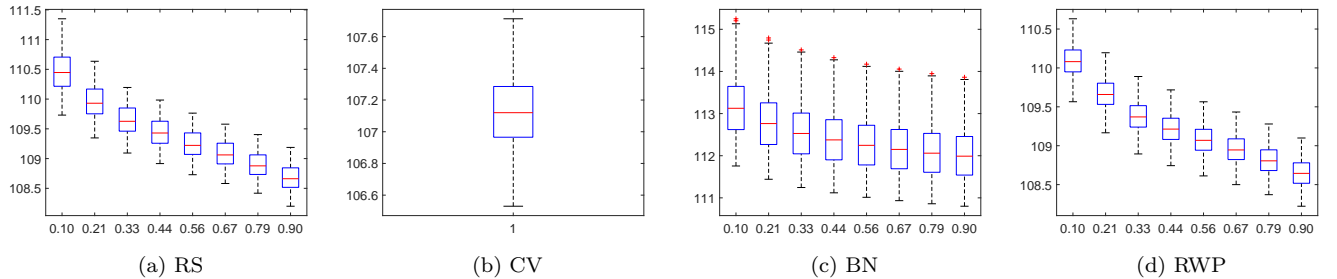


Figure 28: Out of sample loss

C.3.5 $n = 600$

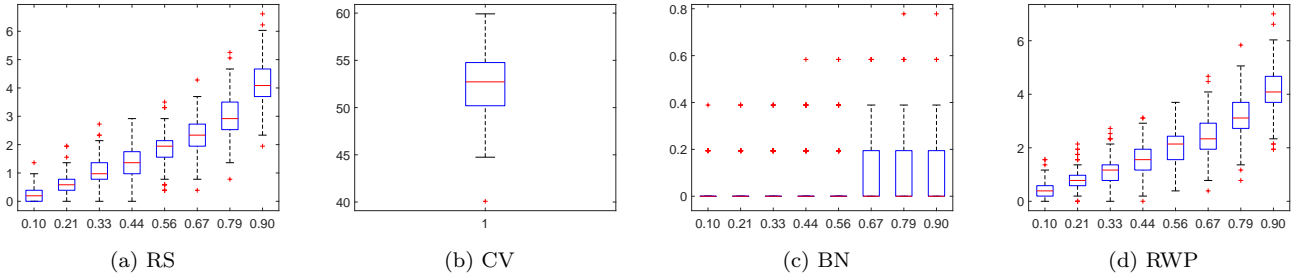


Figure 29: True positive rate (%)

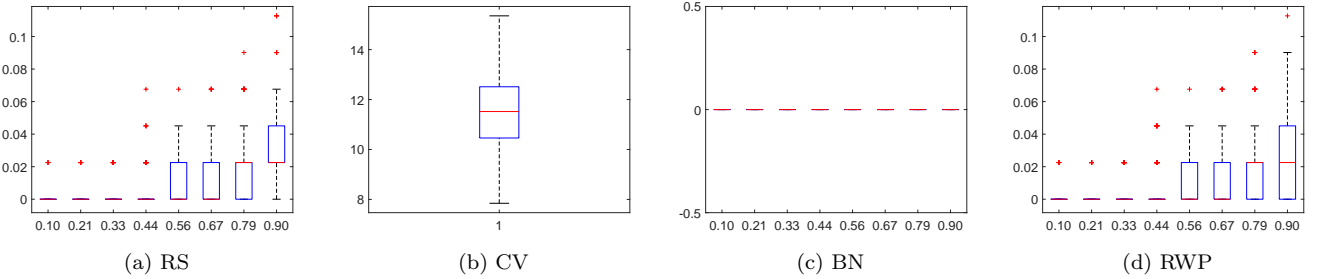


Figure 30: False positive rate (%)

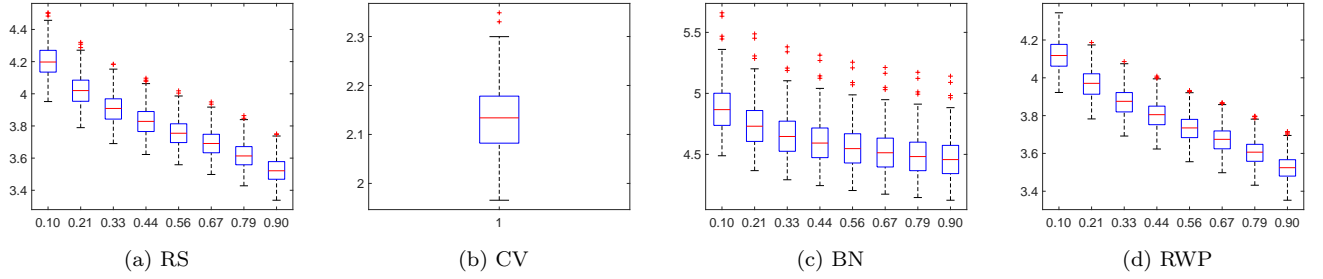


Figure 31: Stein's loss

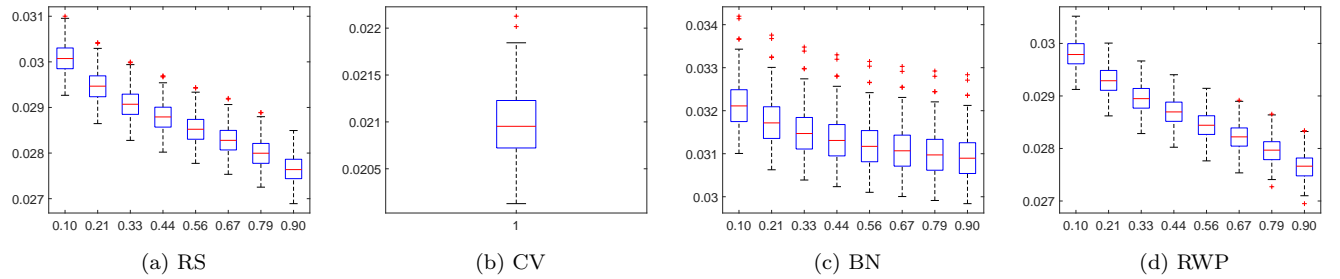


Figure 32: Norm of difference of (inverse) covariances

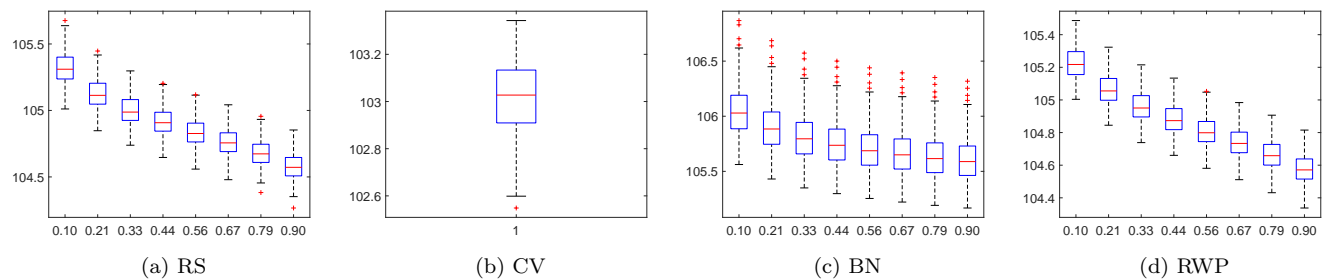


Figure 33: Out of sample loss

C.3.6 $n = 1000$

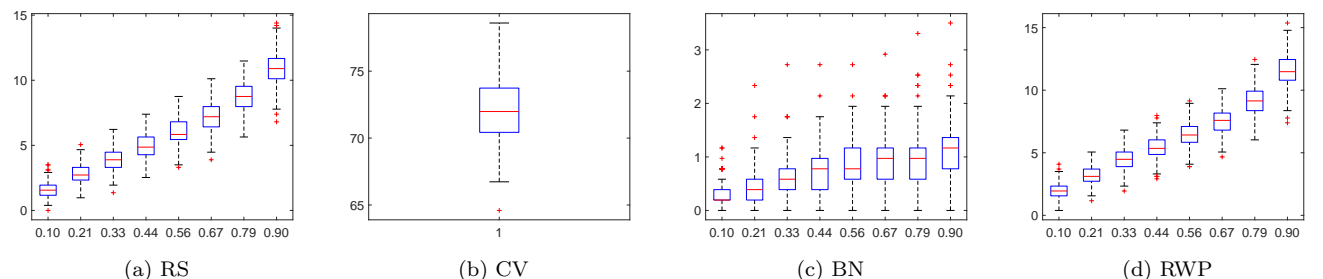


Figure 34: True positive rate (%)

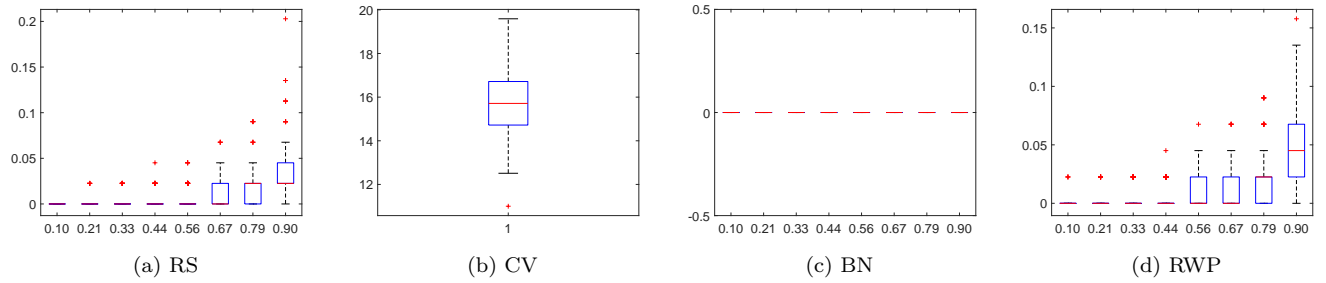


Figure 35: False positive rate (%)

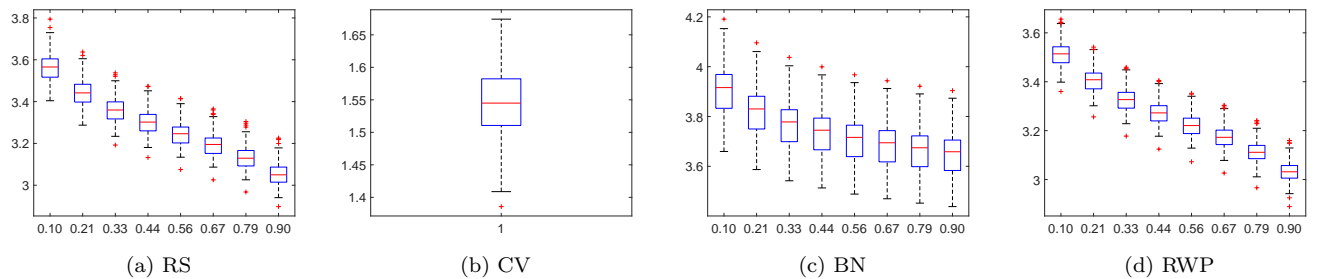


Figure 36: Stein's loss

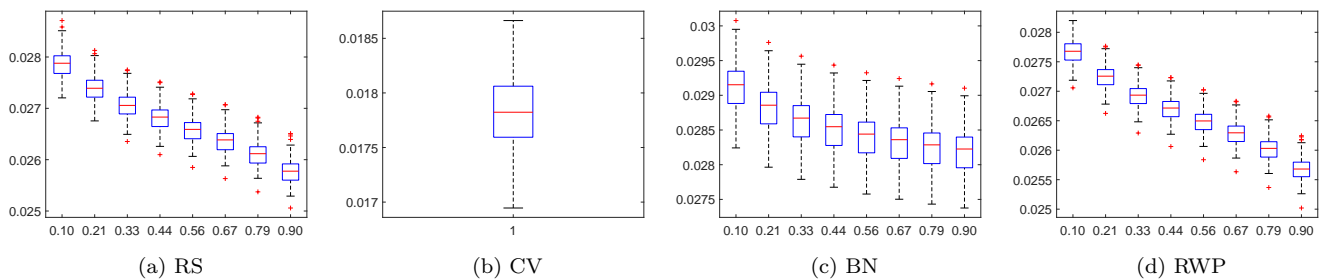


Figure 37: Norm of difference of (inverse) covariances

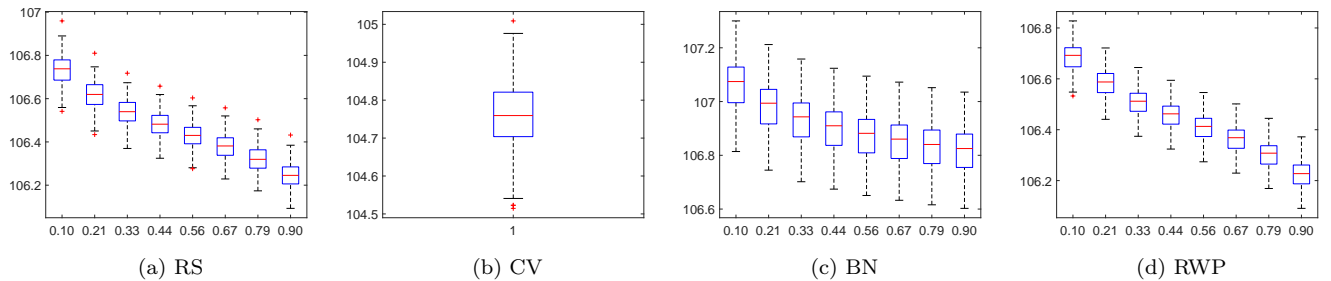


Figure 38: Out of sample loss

C.3.7 $n = 10000$

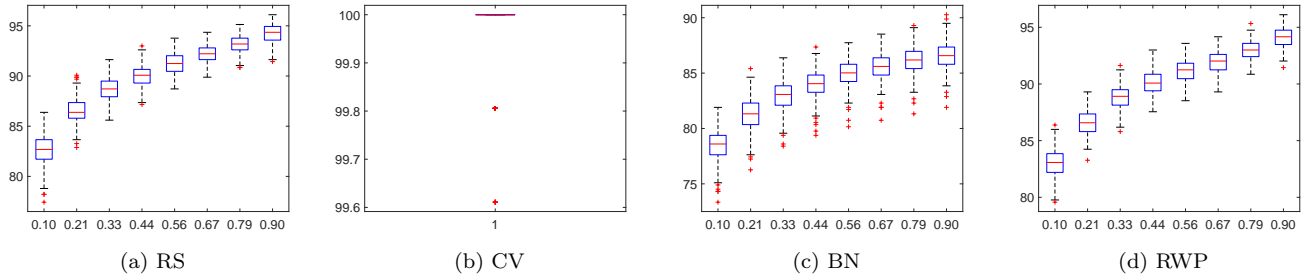


Figure 39: True positive rate (%)

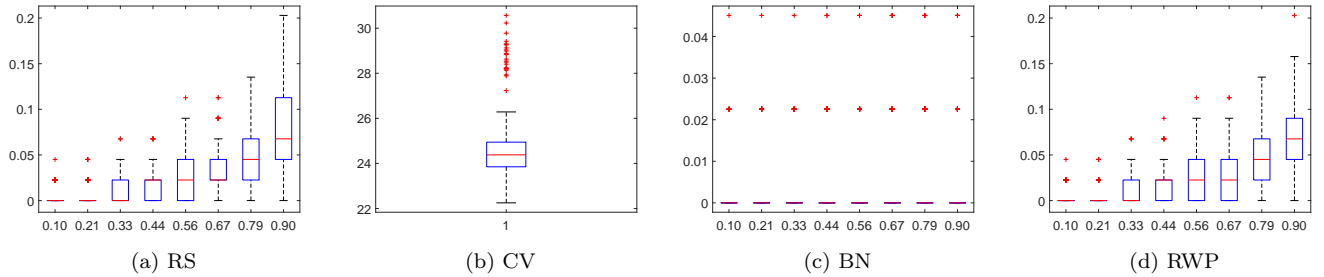


Figure 40: False positive rate (%)

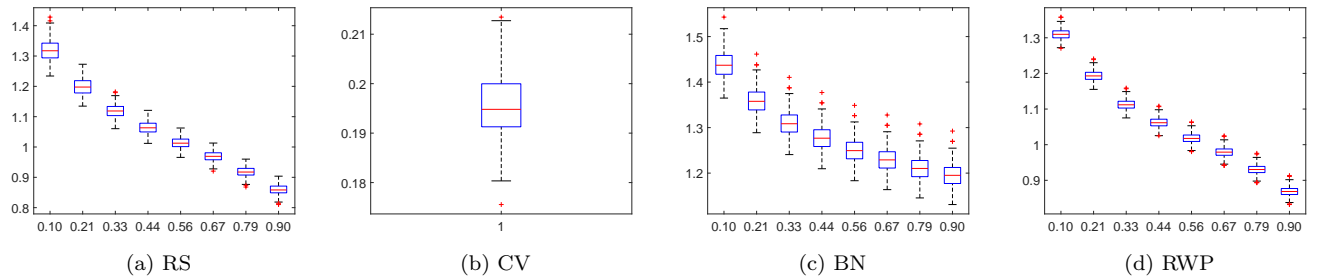


Figure 41: Stein's loss

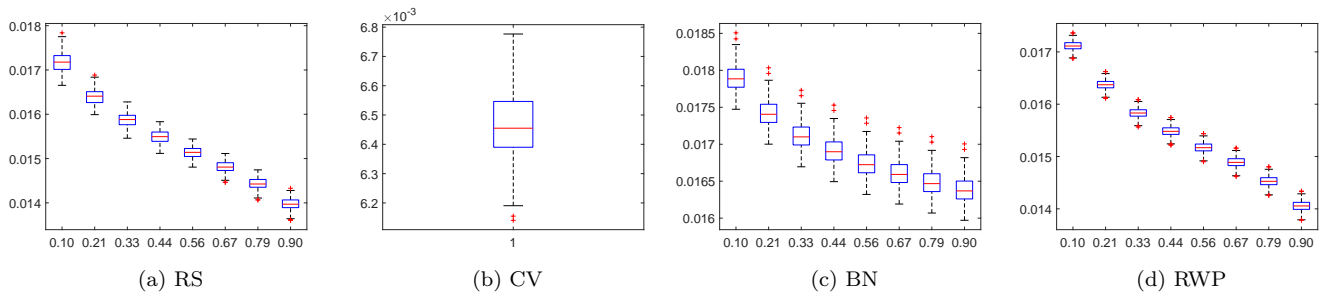


Figure 42: Norm of difference of (inverse) covariances

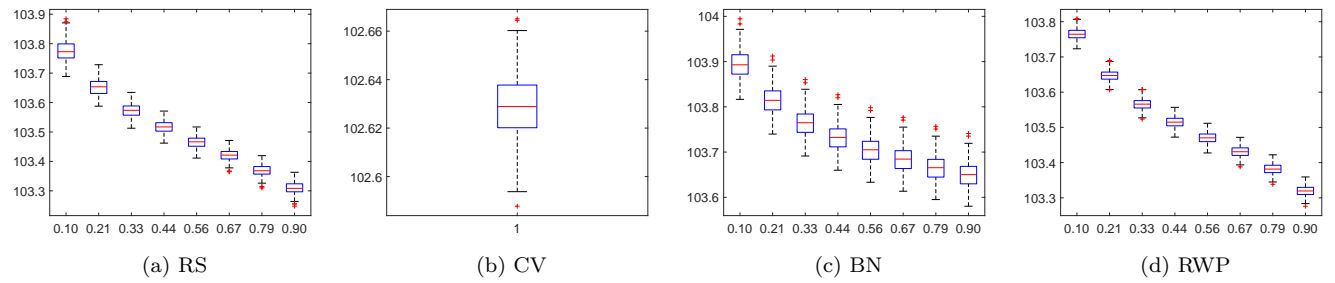


Figure 43: Out of sample loss